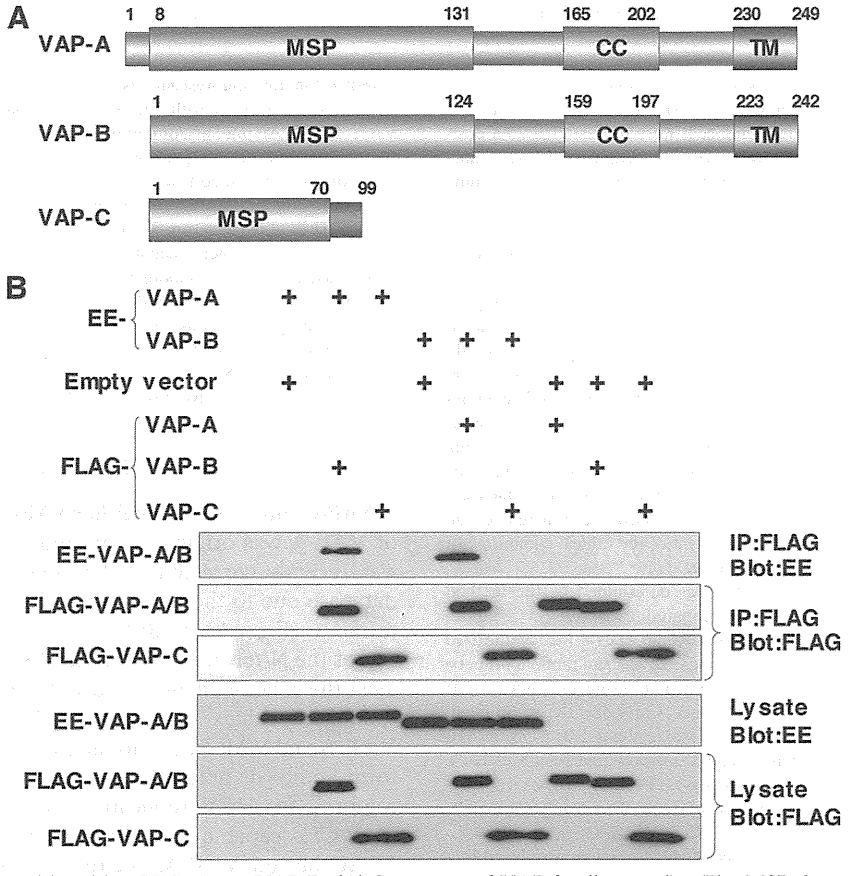

FIG. 1. VAP-C interacts with neither VAP-A nor VAP-B. (A) Structures of VAP family proteins. The MSP domain, the coiled-coil domain, and the TM region are indicated as MSP, CC, and TM, respectively. (B) Interaction among VAP family proteins. The expression plasmids encoding VAP proteins or empty vector (1 μg each) were transfected into 293T cells, FLAG-tagged VAP proteins coexpressed with EE-tagged VAP-A or VAP-B were immunoprecipitated (IP) with anti-FLAG antibody, and the resulting precipitates were examined by immunoblotting using anti-FLAG or anti-EE antibody. One percent of the volume of the lysate was used as an input control. The data in each panel are representative of the results of three independent experiments. +, present.

other host proteins, including VAMP and tubulin, is independent of the FFAT motif (16, 36, 38, 50). The third subtype of VAP is VAP-C, which is an alternative spliced isoform of VAP-B, consisting of the N-terminal half of the MSP domain and the subtype-specific 29 amino acids (Fig. 1A). However, its tissue distribution and physiological function remain largely unknown.

Glutathione *S*-transferase pulldown and immunoprecipitation analyses revealed that both VAP-A and VAP-B interact with NS5B and NS5A through the MSP domain and the coiled-coil domain, respectively (9, 44), and the MSP domains of VAP-A and VAP-B exhibit 82.3% homology. Although VAP-C possesses the N-terminal-half region of the MSP domain of VAP-B, the biological significance of VAP-C in the propagation of HCV has not yet been clarified. In this study, we examined the expression of VAP-C in human tissues and the effects of VAP-C expression on the RNA replication, translation, and particle formation of HCV.

MATERIALS AND METHODS

Cell lines. Cells of the human hepatoma cell line Huh-7, cell line Huh7OK1, and embryonic kidney cell line 293T were maintained in Dulbecco's modified Eagle's medium (DMEM) (Sigma, St. Louis, MO) containing 10% fetal calf serum (FCS) and nonessential amino acids (NEAA), while Huh 9-13 cells, which possess a subgenomic HCV RNA replicon of genotype 1b (21), were cultured in DMEM supplemented with 10% FCS, NEAA, and 1 mg/ml G418. The Huh7OK1 cell line exhibits the highest efficiency of propagation of strain JFH1 virus, as described previously (35). All cell lines were cultured at 37°C in a humidified atmosphere with 5% CO_2.

Antibodies. Chicken anti-human VAP-B antibody was described previously (9). Rabbit anti-human VAP-C antibody was prepared by immunization using synthetic peptides of the amino acid residues from 86 to 98, QPHFSISPNW EGR, which region does not share the homology to VAP-A and VAP-B. The mouse monoclonal antibody to human VAP-A was purchased from BD Pharmingen (San Diego, CA). Mouse monoclonal antibodies to influenza virus hemagglutinin (HA) and the GluGlu (EE) tag were from Covance (Richmond, CA). Mouse and rabbit anti-FLAG antibodies and mouse anti-β-actin monoclonal antibody were from Sigma. Rabbit polyclonal antibody to NS5A was prepared as described previously (34). Mouse anti-NS5A monoclonal antibody was from Austral Biologicals (San Ramon, CA).

Plasmids. A cDNA clone encoding NS5A was amplified from HCV genotype 1b strain J1 (9) (GenBank database accession number D89815) by PCR, using *Pfu* turbo DNA polymerase (Stratagene, La Jolla, CA). The fragments were then cloned into the appropriate sites in pEF-FLAG pGBK puro (13). The DNA fragment encoding NS5B of the J1 strain was generated by PCR and cloned into pCAGGs-PUR (31). The DNA fragment encoding human VAP-A was amplified by PCR from a human fetal-brain library (Clontech, Palo Alto, CA) and was introduced into pEF-FLAG pGBK puro and pEF-EE hygro (13), as described previously (9). A DNA fragment encoding VAP-C was amplified from cDNA of hepatoma cell line Huh-7 and was introduced into pEF-FLAG pGBK puro. Pro^{56}-to-Ser (P56S) mutants of VAPs were generated by site-directed mutagen-

esis (11). All PCR products were confirmed by sequencing with an ABI Prism 3130 genetic analyzer (Applied Biosystems, Tokyo, Japan).

Transfection, immunoblotting, and immunoprecipitation. Cells were seeded onto a six-well tissue culture plate 24 h before transfection. The plasmids were transfected into cells by liposome-mediated transfection using TransIT LT1 (Mirus Bio, Madison, WI). These transfected cells were harvested at 36 h posttransfection, washed three times with 1 ml of ice-cold phosphate-buffered saline (PBS), and suspended in 0.2 ml lysis buffer (20 mM Tris-HCl, pH 7.4, containing 135 mM NaCl and 1% Triton X-100) supplemented with protease inhibitor cocktail (Roche, Indianapolis, IN). The cell lysates were sonicated at 4°C for 5 min, incubated for 30 min at 4°C, and centrifuged at 15,000 rpm for 30 min at 4°C. The supernatant was subjected to immunoprecipitation analyses as described previously (27). The immunoprecipitated proteins were boiled in 30 μl of loading buffer and then subjected to sodium dodecyl sulfate–12.5% polyacrylamide gel electrophoresis. The proteins were transferred to polyvinylidene difluoride membranes (Millipore, Bedford, MA) and then reacted with primary antibody and secondary horseradish peroxidase-conjugated antibody. The immunocomplexes were visualized with Super Signal West Femto substrate (Pierce, Rockford, IL) and detected by using an LAS-3000 image analyzer (Fujifilm, Tokyo, Japan). The distribution of VAPs in human organs was determined by using premade human tissue lysates (Protein medleys; Clonetech), which are aliquots of various organ lysates prepared from samples from several people, and liver tissues obtained during surgery after approval of the ethical committee of Kyushu University Graduate School of Medicine.

Real-time PCR. The HCV genomic RNA was determined by the method described previously (40). Total RNA was prepared from cells by using an RNeasy mini kit (Qiagen, Tokyo, Japan). First-strand cDNA was synthesized using an RNA LA PCR kit (Takara Bio, Inc., Shiga, Japan) and random primers. Expression of the appropriate gene was estimated by using platinum SYBR green quantitative PCR SuperMix UDG (Invitrogen, Carlsbad, CA) according to the manufacturer's protocol. Fluorescent signals were estimated by using an ABI Prism 7000 system (Applied Biosystems). The 5′ untranslated region of HCV and the glyceraldehyde-3-phosphate dehydrogenase (GAPDH) mRNA were amplified using primer pairs described previously (40). The amount of HCV genomic RNA was normalized with that of GAPDH mRNA.

Focus-forming assay. The viral RNA of the JFH1 strain was introduced into the Huh7OK1 cell line according to the method of Zhong et al. (51). The culture supernatant was collected at 7 days posttransfection and used as the infectious HCV particles. Huh7OK1 cells in DMEM containing 10% FCS were seeded at 5×10^4 cells per well into a 24-well plate 12 h before infection. The cells were infected with the JFH1 strain at a multiplicity of infection (MOI) of 0.05 and incubated at 37°C for 2 h. The medium was replaced with fresh DMEM containing 10% FCS and NEAA at 2 h postinfection. The cells were fixed with 4% paraformaldehyde at 96 h postinfection and permeabilized with PBS containing 0.2% Triton X-100. These fixed and permeabilized cells were stained with the anti-NS5A mouse monoclonal antibody and Alexa Fluor (AF) 488-conjugated antibody to mouse immunoglobulin G (Molecular Probes, Eugene, OR). Clusters of infected cells stained with the NS5A antibody were derived from a single infectious focus, and virus titers were represented as focus-forming units/ml.

Quantification of the HCV core protein by ELISA. The HCV core protein was quantified by using an Ortho HCV antigen enzyme-linked immunosorbent assay (ELISA) test (Ortho Clinical Diagnostics, Tokyo, Japan) according to the manufacturer's instructions. To determine the intracellular expression of core protein, Huh7OK1 cells were infected with the infectious HCV particles described above, lysed with the lysis buffer on ice, and applied to the ELISA after 100- to 10,000-fold dilution with PBS. Total protein was quantified by using a Micro BCA protein assay reagent kit (Pierce). The intracellular and extracellular levels of expression of the core protein were normalized by the total amount of protein.

Effect of the VAP expression on the cap-independent translational activity of the viral IRES. The cDNA fragment encoding a firefly luciferase was excised from a pGL3 basic plasmid (Promega, Madison, WI) and introduced into the downstream region of the *Renilla* luciferase gene of pRL-CMV (cytomegalovirus) (Promega). Then, the cDNA fragments encoding the internal ribosome entry site (IRES) of the HCV strains Con1 and JFH1 were introduced between the *Renilla* and firefly luciferase genes, and the resulting plasmids were designated pRL-CMV-HCVCon1 and pRL-CMV-HCVJFH1, respectively (see Fig. 4A). The IRES region of HCV was replaced with that of poliovirus (PV) or encephalomyocarditis virus (EMCV), and the plasmids designated pRL-CMV-PV and pRL-CMV-EMCV, respectively (see Fig. 4B). Each reporter plasmid was introduced into Huh7OK1 cells that had been transfected with the expression plasmid encoding FLAG-green fluorescent protein (GFP), FLAG–VAP-A, FLAG–VAP-B, or FLAG–VAP-C 24 h previously, and cells were harvested at 48 h posttransfection. Luciferase activities in cells were measured by using a dual-luciferase reporter assay system (Promega). The activity of firefly luciferase was normalized with that of *Renilla* luciferase and represented as relative luciferase activity (RLU).

Indirect immunofluorescence assay. The Huh 9-13 cells were cultured on glass slides and transfected with the expression plasmids encoding FLAG-tagged VAPs, P56S VAP mutants, or empty vector. The resulting cells were fixed at 72 h posttransfection with 4% paraformaldehyde in PBS at room temperature for 30 min. After being washed twice with PBS, cells were permeabilized for 20 min at room temperature with PBS containing 0.25% saponin and blocked with PBS containing 1% bovine serum albumin (BSA-PBS) for 60 min at room temperature. The cells were then incubated with BSA-PBS containing rabbit anti-FLAG and mouse anti-NS5A antibodies at 37°C for 60 min, washed three times with PBS containing 1% Tween 20 (PBS-T), and incubated with BSA-PBS containing AF 488-conjugated goat anti-rabbit immunoglobulin G and AF 594-conjugated goat anti-mouse antibodies at 37°C for 60 min. Finally, the cells were washed three times with PBS-T and observed with a FluoView FV1000 laser-scanning confocal microscope (Olympus, Tokyo, Japan).

RESULTS

VAP-C interacts with neither VAP-A nor VAP-B. The length of VAP-A was originally reported to be 242 amino acids but was recently corrected to 249 amino acids in the GenBank database due to the detection of 7 extra amino acids in the N terminus (Fig. 1A). VAP-C is a splicing variant of VAP-B that shares the N-terminal half of the MSP domain with VAP-B but lacks the coiled-coil motif and TM region (Fig. 1A). The region spanning residues 71 to 99 of VAP-C exhibits no homology to VAP-A and VAP-B, due to the frameshift. VAP-A and VAP-B form homo- or heterodimers via their TM domains, which is required for HCV replication (9, 44). To examine whether VAP-C is capable of interacting with VAP-A and VAP-B, FLAG-tagged VAP-A, -B, or -C was coexpressed with EE-tagged VAP-A or -B in 293T cells and was immunoprecipitated with the anti-FLAG antibody. Although EE-tagged VAP-A and VAP-B were coprecipitated with FLAG-tagged VAP-B and VAP-A, as reported previously, FLAG–VAP-C was precipitated with neither EE–VAP-A nor EE–VAP-B (Fig. 1B). These results indicate that VAP-C does not interact with VAP-A and VAP-B.

VAP-C binds to NS5B and interrupts the interaction of VAP-A and VAP-B with NS5B. VAP-A and VAP-B were identified as NS5A-binding proteins by yeast two-hybrid screening (9, 44). The coiled-coil domains of VAP-A and VAP-B were involved in the binding to NS5A, contributing to the efficiency of HCV replication (9, 44). However, VAP-C does not have the coiled-coil domain (Fig. 1A) and, therefore, VAP-C was expected not to interact with NS5A. To examine whether or not interaction between VAP-C and NS5A actually occurred, HA-tagged NS5A was coexpressed with FLAG-tagged VAP-A, -B, or -C in 293T cells and was immunoprecipitated with anti-HA antibody (Fig. 2). The results showed that the expression level of FLAG–VAP-C in the transfected cells was comparable to that of FLAG–VAP-A or FLAG–VAP-B (Fig. 2A, left). Although FLAG-tagged VAP-A and VAP-B were coprecipitated with HA-NS5A, no precipitation of FLAG–VAP-C with NS5A was detected (Fig. 2A, right), indicating that VAP-C does not interact with NS5A.

The RNA-dependent RNA polymerase NS5B was shown to interact with VAP-A through the MSP domain (44). The region spanning residues 1 to 70 of VAP-C is the same as the N-terminal-half region of the MSP domain of VAP-B and exhibits 77% homology to that of VAP-A (Fig. 1A). To exam-

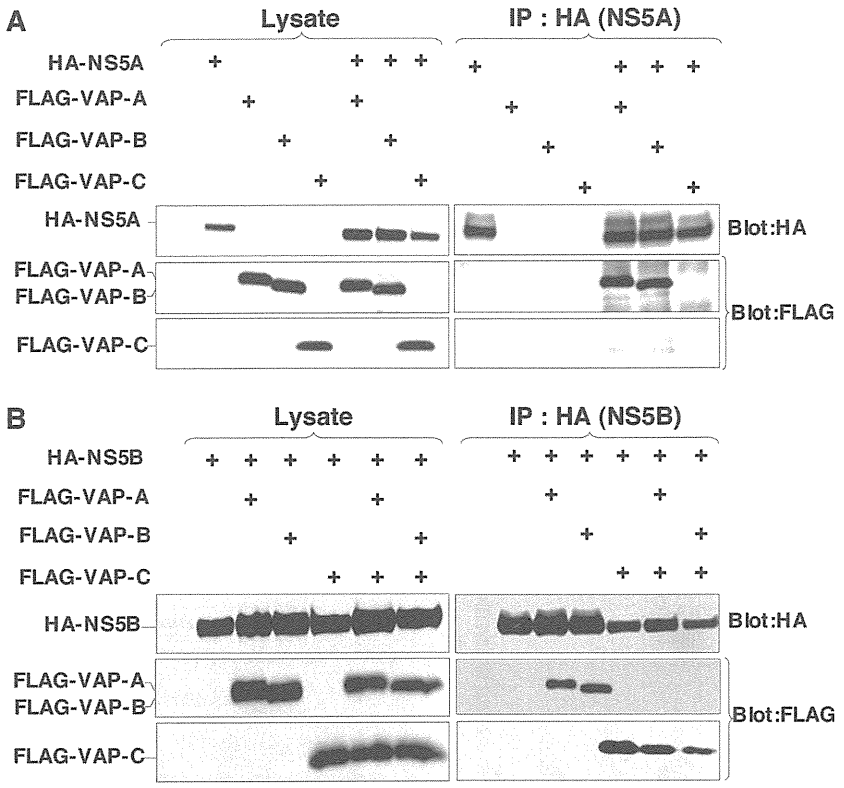

FIG. 2. VAP-C binds to NS5B but not NS5A and interrupts the interaction of VAP-A and VAP-B with NS5B. (A) The expression plasmids encoding NS5A or VAP proteins (1 μg each) were transfected into 293T cells after adjusting the total amounts of DNA to 2.0 μg with empty plasmid. HA-tagged NS5A was coexpressed with either FLAG-tagged VAP-A, VAP-B, or VAP-C in 293T cells and immunoprecipitated (IP) with anti-HA antibody, and the resulting precipitates were immunoblotted using anti-FLAG or anti-HA antibody. (B) The expression plasmids encoding NS5B or VAP proteins (1 μg each) were transfected into 293T cells after adjusting the total amounts of DNA to 3.0 μg with empty plasmid. HA-tagged NS5B was coexpressed with either FLAG-tagged VAP-A or VAP-B in the presence or absence of FLAG-tagged VAP-C in 293T cells and immunoprecipitated (IP) with anti-HA antibody, and the resulting precipitates were immunoblotted using anti-FLAG or anti-HA antibody. One percent of the lysate was used as an input control. The data in each panel are representative of the results of three independent experiments. +, present.

ine whether VAP-C is capable of interacting with NS5B, as are VAP-A and VAP-B, HA-NS5B was coexpressed with FLAG–VAP-A, FLAG–VAP-B, or FLAG–VAP-C in 293T cells and was immunoprecipitated with anti-HA antibody (Fig. 2B). Although substantial amounts of FLAG-tagged VAP-A, VAP-B, and VAP-C were coexpressed, and although all three were coprecipitated with HA-NS5B at comparable levels, the interaction of HA-NS5B with FLAG-tagged VAP-A or VAP-B was impaired by the coexpression of VAP-C, while FLAG–VAP-C was coprecipitated with HA-NS5B instead of FLAG-tagged VAP-A or VAP-B. These results suggest that VAP-C is capable of binding to NS5B and that the expression of VAP-C interrupts the interactions of NS5B with VAP-A and VAP-B.

Expression of VAP-C impairs the replication of HCV. VAP-A and VAP-B are known to support the replication of HCV RNA (2, 7). To examine the effect of VAP-C on the replication of HCV, FLAG–VAP-C was expressed in HCV replicon cells, Huh 9-13, in which a subgenomic HCV RNA of the genotype 1b strain Con1 was autonomously replicating. Huh 9-13 cells transfected with a plasmid encoding FLAG–VAP-C were harvested periodically up to 72 h posttransfection. The levels of replication of viral RNA and expression of NS5A were determined by real-time PCR and immunoblotting, respectively (Fig. 3). The expression of VAP-C reduced the intracellular RNA of the subgenomic HCV replicon in accordance with the incubation period after transfection with the expression plasmid of FLAG–VAP-C; the empty plasmid did not reduce the intracellular RNA (Fig. 3A). The expression of NS5A was gradually decreased and was undetectable at 72 h posttransfection, in contrast to the increase of VAP-C expression (Fig. 3B).

Next, to determine the effects of VAP-C expression on the replication of HCV, Huh 9-13 cells were transfected with 0 to 4 μg of the expression plasmid encoding VAP-A, VAP-B, or VAP-C and the replication of the subgenomic HCV RNA was determined at 48 h posttransfection. Although the HCV replicon cells transfected with 4 μg of a plasmid encoding FLAG–VAP-B exhibited enhancement of the RNA replication, those transfected with an equivalent amount of plasmid encoding FLAG–VAP-A or empty vector showed a slight reduction of HCV RNA replication. In contrast, the replicon cells transfected with a plasmid encoding FLAG–VAP-C exhibited a clear reduction of the HCV RNA replication in a dose-dependent manner (Fig. 3C). The expression of FLAG-tagged VAP-A, VAP-B, or VAP-C in the replicon cells was increased in correspondence with the amount of the transfected plasmid

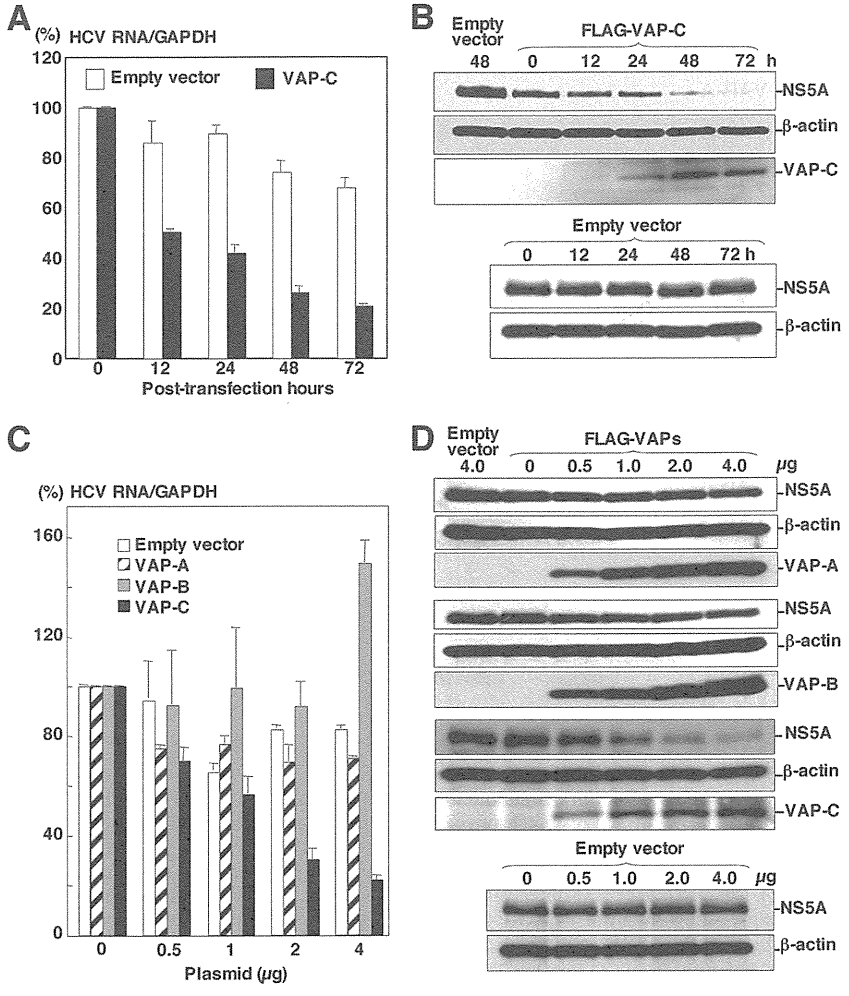

FIG. 3. Expression of VAP-C impairs the replication of HCV. (A) HCV replicon cells (Huh 9-13) were transfected with 4 μg of the expression plasmids encoding FLAG-tagged VAP-C or empty vector, and the level of intracellular HCV RNA was determined at 0, 12, 24, 48, or 72 h posttransfection by real-time PCR after normalization with GAPDH mRNA. The value of HCV RNA at 0 h posttransfection in the cell line transfected with the empty plasmid is represented as 100%. Data in this panel are shown as means ± standard deviations. (B) Huh 9-13 cells were transfected with 4 μg of the plasmid encoding FLAG-tagged VAP-C or empty plasmid, and the levels of expression of NS5A, β-actin, and VAP-C were determined at 0, 12, 24, 48, or 72 h posttransfection by immunoblotting using anti-NS5A, anti-β-actin, or anti-FLAG tag antibody. (C) Huh 9-13 cells were transfected with 0 to 4 μg of the plasmids encoding FLAG-tagged VAP-A, VAP-B, or VAP-C or empty vector, and the level of intracellular HCV RNA was determined at 72 h posttransfection as described for panel A. Data in this panel are shown as means ± standard deviations. (D) Huh 9-13 cells treated as described for panel C were harvested at 72 h posttransfection, and the levels of expression of NS5A, β-actin, VAP-A, VAP-B, and VAP-C were determined by immunoblotting. The data in each panel are representative of the results of three independent experiments.

(Fig. 3D), and the expression of NS5A was suppressed in accordance with the expression of FLAG–VAP-C, whereas the expression of FLAG–VAP-A and FLAG–VAP-B exhibited no effect on the expression of NS5A. These results suggest that the expression of VAP-C impairs the replication of HCV RNA.

VAP-C exhibits no effect on the IRES-dependent translation. The expression of VAP-C was shown to suppress the replication of the HCV RNA replication of the replicon cells. Next, to determine the effect of VAPs on the translation of HCV RNA, the reporter plasmid encoding the *Renilla* luciferase gene under the control of the CMV promoter and the firefly luciferase gene under the IRES of HCV, PV, or EMCV, in that order, was prepared as shown in Fig. 4. These reporter plasmids were introduced into Huh7OK1 cells 24 h after transfection of the expression plasmids encoding VAP-A, VAP-B, or VAP-C and harvested at 48 h posttransfection, and then the RLUs were determined. Although VAP-C exhibited a slight increase in the IRES-dependent translations of the HCV strains Con1 and JFH1, no significant effect of the expression of the VAPs on the HCV IRES-dependent translation was observed (Fig. 4A). Similarly, the expression of each of the VAPs in Huh7OK1 cells exhibited no significant effect on the IRES-dependent translation of PV or EMCV (Fig. 4B). These results indicate that the suppression of HCV RNA replication by the expression of

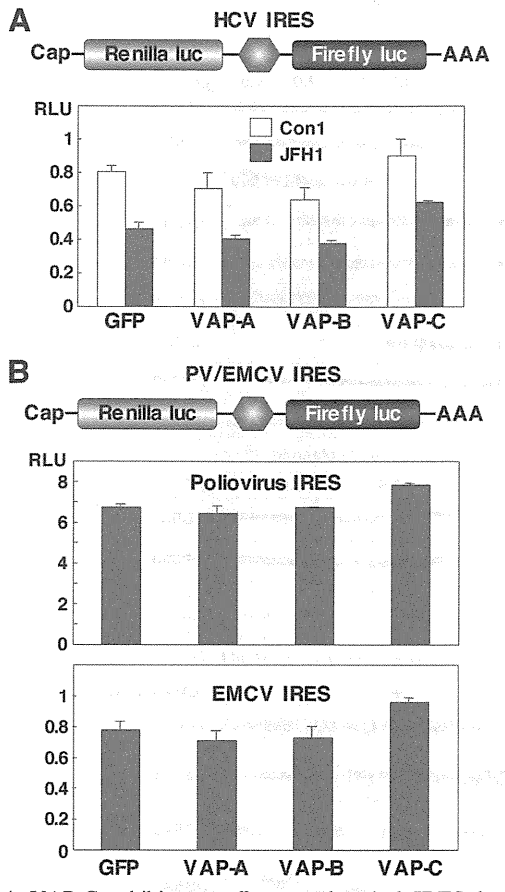

FIG. 4. VAP-C exhibits no effect on the viral IRES-dependent translation. (A) Top: structure of a reporter plasmid encoding the *Renilla* luciferase gene under the control of the CMV promoter and the firefly luciferase gene under the HCV IRES, in order. Bottom: the reporter plasmid was introduced into Huh7OK1 cells 24 h after transfection of the expression plasmids encoding VAP-A, VAP-B, or VAP-C, the cells harvested at 48 h posttransfection, and the RLUs determined after standardization with the expression of *Renilla* luciferase. (B) Top: structure of a reporter plasmid encoding the *Renilla* luciferase gene under the control of the CMV promoter and the firefly luciferase gene under the PV or EMCV IRES, in order. Bottom: each of the reporter plasmids was introduced into Huh7OK1 cells, and the RLU values were determined as described for panel A. Data in this figure are shown as the means ± standard deviations.

VAP-C was not due to the suppression of the IRES-dependent translation of the viral RNA genome.

VAP-C impairs HCV propagation. To examine the effect of VAP expression on HCV propagation, Huh7OK1 cells transfected with the expression plasmids encoding VAP-A, VAP-B, or VAP-C were infected with JFH1 virus, and the levels of production of the viral RNA, core protein, and infectious particles were determined at 96 h postinfection. The production of intracellular and extracellular viral RNA was increased up to 10 to 30 times and 2 to 3 times, respectively, by the expression of VAP-A or VAP-B whereas it was clearly decreased in a dose-dependent manner by the expression of VAP-C (Fig. 5A). Although the extracellular core protein was increased from 0.6 to 2.6 nmol/liter by the expression of VAP-A or VAP-B, as seen in the production of viral RNA, the intracellular core protein showed only a marginal increase (40 to 65 nmol/liter) (Fig. 5A). Although the reason for the discrepancy between the intracellular production of viral RNA and core protein is not known at the moment, some mechanisms other than RNA translation might be involved, because VAP expression exhibited no effect on the HCV IRES-dependent translation, as shown in Fig. 4A. In contrast to the enhancement of core protein production by the expression of VAP-A or VAP-B, the expression of VAP-C significantly reduced both the intracellular and extracellular expression of the core protein (Fig. 5A). Furthermore, the production of infectious particles in the culture supernatants of Huh7OK1 cells infected with JFH1 virus was slightly enhanced by the expression of VAP-A or VAP-B, whereas it was suppressed by the expression of VAP-C (Fig. 5A). To further confirm the effects of VAPs on the expression of HCV proteins, Huh7OK1 cells transfected with various amounts of the expression plasmids of VAP-A, VAP-B, or VAP-C and infected with the JFH1 virus were examined by immunoblotting (Fig. 5B). Although the expression of VAP-A or VAP-B exhibited no effect on NS5A expression, VAP-C expression clearly decreased the expression of NS5A in a dose-dependent manner. These results clearly indicate that the expression of VAP-C negatively regulates HCV propagation. Overexpression of VAP-C did not affect the endogenous expression of VAP-A or VAP-B (Fig. 5C), suggesting that suppression of HCV propagation by VAP-C is not due to the reduction of VAP-A or VAP-B expression.

Lack of VAP-C expression in human livers. VAP-C consists of the first 70 amino acid residues of VAP-B and the subtype-specific 29 amino acid residues derived from frameshift (Fig. 1A). The VAP-C-specific antibody generated by immunization with the peptide corresponding to the residues from 86 to 98 clearly detected VAP-C but neither VAP-A nor VAP-B in cells transfected with expression plasmids encoding FLAG-tagged VAP-A, VAP-B, or VAP-C (Fig. 6A). To determine the distribution of VAPs in human organs, the pool lysates of various organs prepared from several people were examined by immunoblotting (Fig. 6B). Expression of VAP-A was detected clearly in the kidney, lung, prostate, and liver; slightly in the duodenum, uterus, vagina, and bladder; and barely in the small intestine and stomach. VAP-B was detected clearly in the bladder, kidney, and prostate and slightly in the duodenum, small intestine, uterus, vagina, and liver. Expression of VAP-C was detected clearly in the stomach, uterus, kidney, and bladder; slightly in the duodenum, small intestine, and prostate; and barely detected in the vagina, lung, and liver. Several bands smaller than the expected size of VAP-C were observed in the stomach, duodenum, small intestine, uterus, vagina, prostate, and bladder. Because the main target of HCV replication is thought to be the liver, we next examined the expression of VAPs in individual human liver samples. VAP-A and VAP-B were clearly detected in the liver tissues obtained from chronic hepatitis C patients and a healthy donor, but no expression of VAP-C was detected (Fig. 6C). These results suggest that the expression of VAP-C may participate in the determination of tissue tropism of HCV propagation.

Substitution of Ser for Pro^{56} in VAPs leads to suppression of HCV replication. A single mutation of Pro^{56} to Ser (P56S) of VAP-B has been reported to be highly associated with amyotrophic lateral sclerosis (ALS), and the P56S mutation of VAP-B but not of VAP-A has been shown to induce large

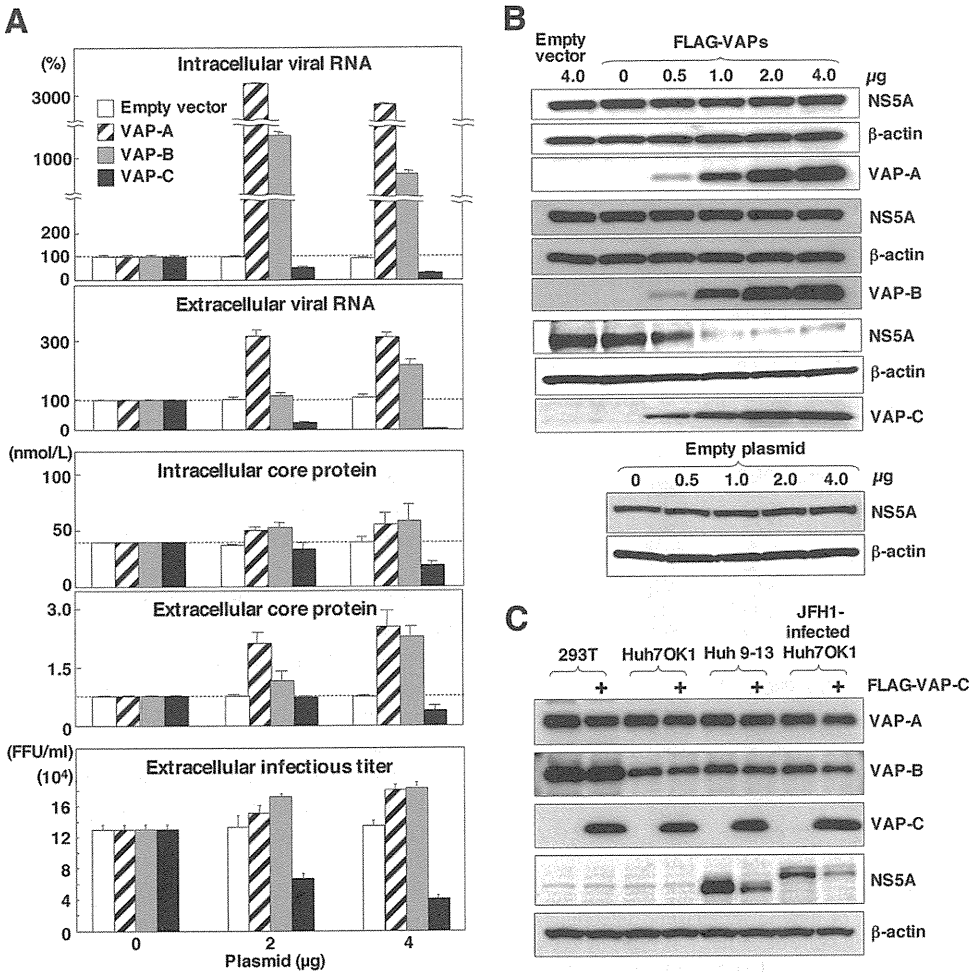

FIG. 5. VAP-C impairs HCV propagation but does not affect endogenous expression of VAP-A or VAP-B. Huh7OK1 cells transfected with 0 to 4 μg of plasmid encoding the FLAG-tagged VAP-A, VAP-B, or VAP-C or empty vector were infected with strain JFH1 at an MOI of 0.05 at 14 h posttransfection and then harvested at 96 h postinfection. (A) The intracellular and extracellular expression levels of viral RNA (top) and core protein (middle) were determined by real-time PCR and ELISA, respectively. Infectious viral titers in the culture supernatants were determined by focus-forming assay (bottom). Data in this panel are shown as the means ± standard deviations. (B) The expression levels of NS5A, β-actin, VAP-A, VAP-B, and VAP-C were determined by immunoblotting using anti-NS5A, anti-β-actin, or anti-FLAG tag antibody. (C) The embryonic kidney cell line (293T), the cured hepatoma cell line (Huh7OK1), and the replicon cell line (Huh 9-13) were transfected with 2 μg of the plasmid encoding FLAG-tagged VAP-C (+) or empty plasmid. In the case of the infected cells, Huh7OK1 cells were infected with strain JFH1 at an MOI of 0.05, reseeded onto the tissue culture plate at 96 h postinfection, and then transfected with 2 μg of the plasmids. These cells were harvested at 36 h posttransfection and examined by immunoblotting using antibodies to VAP-A, VAP-B, FLAG, NS5A, and β-actin. The data in each panel are representative of the results of three independent experiments.

aggregations of ER in culture cells and to sequester the wild-type protein into ubiquitinated inclusions (29, 37). To examine the effects on the replication of HCV of the P56S mutation in VAPs, FLAG-tagged VAP mutants were expressed in the HCV replicon cells. RNA replication of the subgenomic replicon in Huh 9-13 cells was impaired by the expression of each of the mutant VAPs (Fig. 7A, left). The expression of NS5A in the replicon cells was decreased by the expression of the mutant VAPs in a dose-dependent manner (Fig. 7A, right). Next, to examine the effect of the expression of the P56S VAP mutants on HCV propagation, Huh7OK1 cells expressing the FLAG-tagged VAP mutants were infected with JFH1 virus. The production of intracellular and extracellular viral RNA at 96 h postinfection was decreased by the expression of the P56S mutation in VAPs (Fig. 7B). Although the results of a previous study indicated that the expression of the P56S mutant of VAP-B but not that of VAP-A induced a large aggregation of ER in hamster ovary cell line CHO (37), the P56S mutants of VAP-A and VAP-B but not that of VAP-C exhibited accumulation of membranous aggregates in Huh 9-13 cells (Fig. 7C). These results indicate that the P56S mutation in both VAP-B and VAP-A induces aggregation of ER in human hepatoma cells, which in turn leads to the suppression of HCV propagation.

DISCUSSION

The replication of HCV has been shown to require several host proteins, including VAP-A/VAP-B (6, 9, 44), FBL2 (46), FKBP8 (34), hB-ind1 (40), Hsp90 (28, 34, 45), and cyclophilins

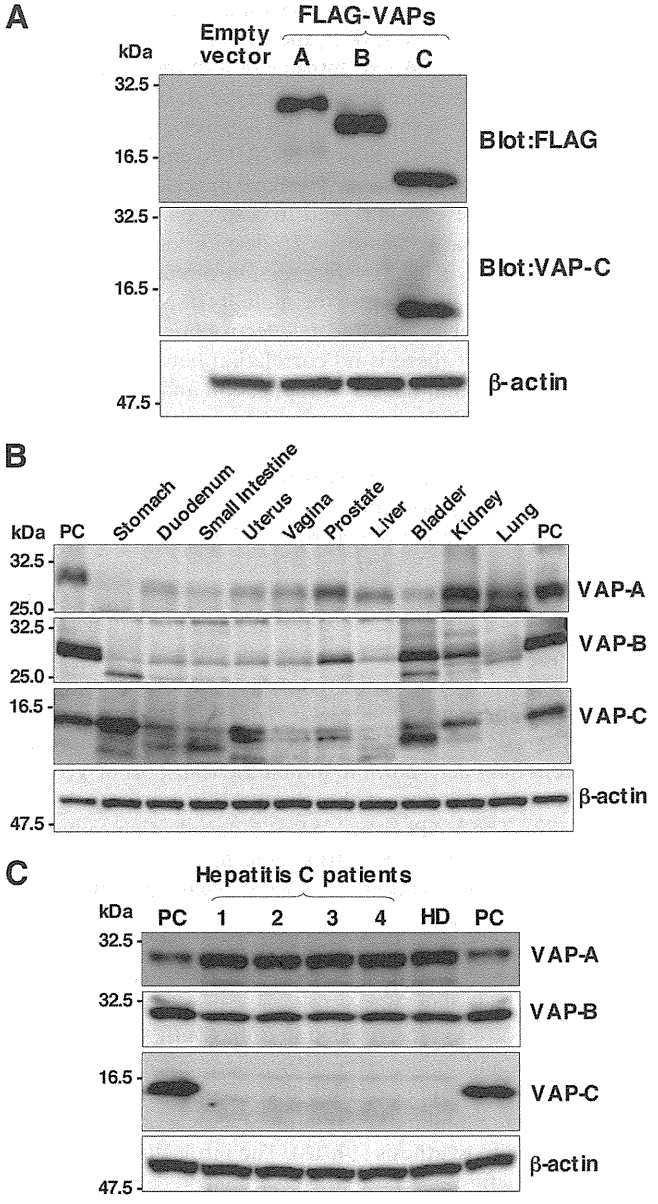

FIG. 6. Distribution of VAPs in human tissues. (A) Anti-VAP-C antibody specifically recognizes VAP-C. Human embryonic kidney 293T cells transfected with expression plasmid encoding FLAG-tagged VAP-A, VAP-B, or VAP-C or empty vector were harvested at 48 h posttransfection and examined by immunoblotting using anti-FLAG tag, anti-VAP-C, and anti-β-actin antibodies. (B) The premade human tissue lysates "Protein medleys" (20 μg each; Clonetech) were examined by immunoblotting using antibodies against VAP-A, VAP-B, VAP-C, or β-actin. (C) Expression of VAP family proteins in human liver tissues. Liver samples obtained from four hepatitis C patients (1 to 4) and one healthy donor (HD) were examined by immunoblotting as described above. The data in each panel are representative of the results of three independent experiments. PC indicates 293T cells transfected with expression plasmid encoding VAP-A, VAP-B, and VAP-C.

(15, 48). VAP-A has been detected in a detergent-resistant membrane fraction that was shown to be capable of replicating HCV RNA in vitro, and the interaction of VAP-A with NS5A is required for the efficient replication of HCV genomic RNA

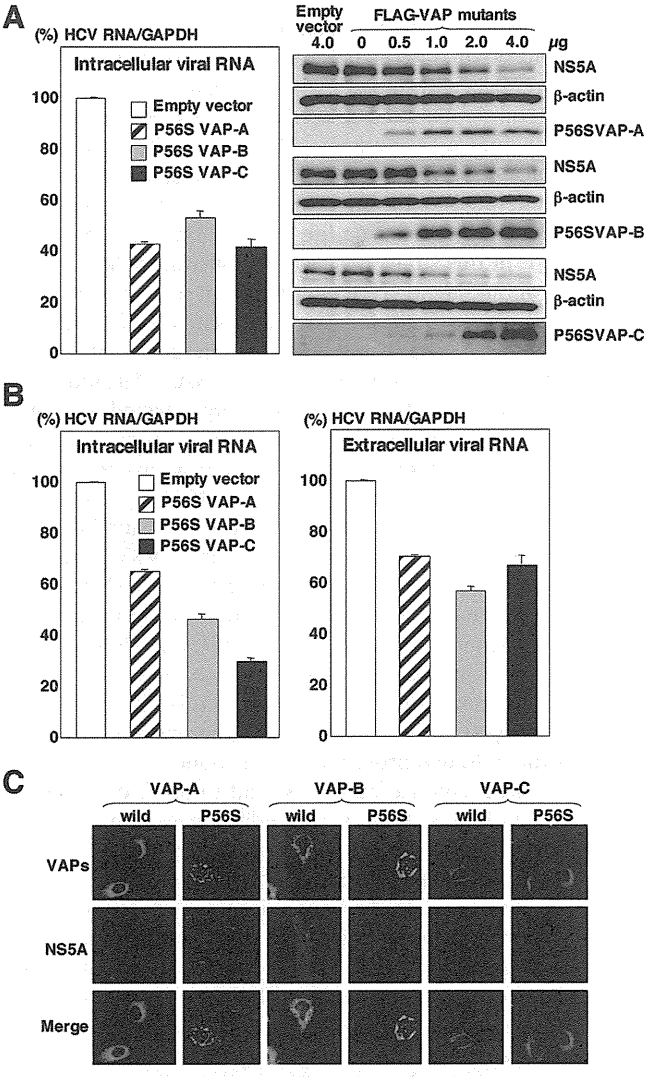

FIG. 7. Substitution of Ser for Pro[56] in VAPs leads to suppression of HCV replication. (A) Left: Huh 9-13 cells were transfected with 4 μg of the expression plasmids encoding FLAG-tagged P56S VAP mutants or empty vector, and the level of intracellular HCV RNA was determined at 72 h posttransfection by real-time PCR after normalization with GAPDH mRNA. The value for HCV RNA at 0 h posttransfection in the cell line transfected with the empty plasmid is represented as 100%. Data in this panel are shown as the means ± standard deviations. Right: Huh 9-13 cells were transfected with 0 to 4 μg of the FLAG-tagged P56S VAP mutant plasmids or empty vector, and the levels of expression of NS5A, β-actin, and the mutant VAPs were determined by immunoblotting at 72 h posttransfection. The data in each panel are representative of the results of three independent experiments. (B) Huh7OK1 cells transfected with 4 μg of the expression plasmids encoding FLAG-tagged P56S VAP mutants or empty vector were infected with strain JFH1 at an MOI of 0.05 at 14 h posttransfection, and the intracellular (left) and extracellular (right) expression levels of viral RNA were determined by real-time PCR after normalization with GAPDH mRNA at 96 h postinfection. Data in this panel are shown as the means ± standard deviations. (C) Levels of expression of wild-type VAPs, P56S mutant VAPs, and NS5A in Huh 9-13 cells at 72 h after transfection with the expression plasmids encoding FLAG-tagged VAPs or P56S VAP mutants were determined by immunofluorescent assay. The data in each panel are representative of the results of three independent experiments.

(2, 7) and is modulated by the phosphorylation of NS5A (4, 6). VAP-B also participates in HCV replication through the formation of homo- and/or heterodimers with VAP-A (9). VAP-A and VAP-B form hetero- and homodimers through their TM regions and interact with NS5A and NS5B through the coiled-coil domain and MSP domain, respectively (9, 44). VAP-C is a splicing variant of VAP-B, consisting of the N-terminal half of VAP-B and the subtype-specific amino acid residues generated by the frameshift. However, the biological significance of VAP-C in the life cycle of HCV has not been determined. In this study, we have demonstrated that VAP-C is capable of binding to HCV NS5B but not to NS5A, VAP-A, and VAP-B due to the lack of the coiled-coil and TM regions. The expression of VAP-C inhibited the interaction of VAP-A and VAP-B with NS5B, impaired the RNA replication and particle formation of HCV, and was barely detected in human liver cells. These results suggest that VAP-C acts as a negative regulator for HCV propagation and is partly involved in the determination of the tissue specificity of HCV replication.

Overexpression of VAP-A but not of VAP-B inhibited the incorporation of the vesicular stomatitis virus (VSV) envelope glycoprotein G (VSV-G) into ER vesicles in CHO cells, resulting in impairment of membrane protein transport from the ER to the Golgi apparatus (37). VAP-B was shown to be involved in the unfolded protein response, which is an ER reaction to suppress the accumulation of misfolded proteins, and the expression of the P56S VAP-B mutant was suggested to nullify the unfolded protein response induced by VAP-B, to produce a large aggregation of ER, and to be involved in the development of ALS (17, 37). These data suggest that VAP-A and VAP-B possess different physiological functions; however, the contributions of the proteins to the life cycle of HCV have not been characterized. The expression of VAP-B but not of VAP-A resulted in an enhancement of the replication of the subgenomic HCV RNA of the genotype 1b strain Con1, whereas the expression of either VAP-A or VAP-B clearly enhanced viral RNA replication in cells infected with the genotype 2a strain JFH1 virus, suggesting that the contributions of VAP-A and VAP-B to viral RNA replication might differ among the genotypes of HCV. The expression of VAP-B or VAP-A enhanced RNA replication in the HCV replicon cells and the secretion of viral RNA, core protein, and infectious particles into the culture supernatants of Huh7OK1 cells infected with JFH1 virus, whereas the expression of these proteins had no effect on the expression of NS5A or on IRES-dependent translation. Thus, further studies will be needed to clarify the molecular mechanisms underlying the posttranslational enhancement of HCV production by the expression of VAP-A and VAP-B. In contrast to the expression of VAP-A and VAP-B, the expression of VAP-C clearly suppressed the RNA replication of both the genotype 1b RNA replicon cells and the genotype 2a strain JFH1 virus, by which both the expression of the viral proteins and the viral particle production were drastically impaired. Furthermore, the expression of the P56S mutants of VAP-A and VAP-B reduced RNA replication in HCV replicon cells and propagation of the JFH1 virus, probably due to the induction of aggregation of the ER. The reason why ER aggregation was induced by the expression of the P56S VAP-A mutant in Huh7 cells but not in CHO cells (17, 37) is not known at the moment.

The phosphorylation state of NS5A was suggested to control the interaction between VAP-A and NS5A and the replication efficiency of HCV RNA (6). Introduction of the adaptive mutations originally identified in the genotype 1b strain Con1 into NS5A of genotype 1a suppressed the hyperphosphorylation of NS5A, potentiated interaction with VAP-A, and enhanced the RNA replication (6). However, we have previously shown that NS5A of genotype 1a could bind to VAP-A and VAP-B at a level similar to that of genotype 1b despite the adaptive mutations (9). In this study, overexpression of each of the VAP proteins exhibited no effect on the mobility of NS5A in sodium dodecyl sulfate-polyacrylamide gel electrophoresis (Fig. 3 and 5), suggesting that there is no correlation between the VAP-dependent regulation of HCV propagation and the phosphorylation state of NS5A.

FKBP8 exhibits peptidyl prolyl *cis-trans* isomerase activity and interacts with NS5A and Hsp90 through the tetratricopeptide repeat (TPR) domain, and these interactions are suggested to be involved in the correct folding of the HCV replication complex (34). Treatment of cells with inhibitors of the ATPase activity of Hsp90, such as geldanamycin and its derivatives, impairs the RNA replication and particle production of HCV (28, 34, 45). The MSP domain of VAP-A was shown to interact with the TPR1 protein, which has a TPR domain and forms the chaperone complex with Hsp90 (22). Knockdown of the TPR1 protein or treatment with Hsp90 inhibitors in mammalian cells has been shown to inhibit the transport of VSV-G, leading to accumulation of the glycoprotein in the Golgi apparatus (22). The VAP-A- or VAP-B-induced enhancement of virus production might be attributable to the recruitment of Hsp90 into the replication complex through the interaction with the MSP domain.

VAP-A is well known to interact through the MSP domain with a number of mammalian and yeast proteins sharing the FFAT motif, including OSBPs, ORPs (20), and CERT (10, 19), and to be involved in the regulation of biosynthesis or trafficking of sterols and lipids. HCV replication and infection have been shown to be regulated by lipid components and to be capable of being inhibited by treatment with several inhibitors targeting lipid biosynthesis (14, 18). The intracellular membranous web structure observed in HCV replicon cells was shown to be resistant to detergent treatment, suggesting that the lipid raft-like structure abundant in cholesterol and sphingolipid is generated by the replication of HCV RNA (2, 24). Therefore, it might be feasible to speculate that VAP-A and VAP-B are involved in the construction of the HCV replication complex consisting of viral proteins and host cellular lipid components and that VAP-C interrupts the VAP-A and VAP-B functions and negatively regulates HCV propagation. Although the molecular mechanisms and the biological significance remain to be clarified, the MSP domain of VAP proteins was processed in human leukocytes and secreted into human serum (43). Further studies are needed to clarify the biogenesis and biological functions of the truncated VAP proteins in the replication of HCV.

In summary, we have shown that VAP-C is capable of suppressing the RNA replication and particle production of HCV by inhibiting the binding of VAP-A and VAP-B to NS5B through the N-terminal half of its MSP domain. The clear suppression of HCV propagation by the expression of VAP-C

further suggests the possibility of developing a novel therapeutic measure to eliminate HCV by the exogenous expression of VAP-C in the hepatocytes of chronic hepatitis C patients.

ACKNOWLEDGMENTS

We thank H. Murase for her secretarial work. We also thank R. Bartenschlager and T. Wakita for providing cell lines and plasmids.

This work was supported in part by grants-in-aid from the Ministry of Health, Labor, and Welfare; the Ministry of Education, Culture, Sports, Science, and Technology; the Global Center of Excellence Program; and the Foundation for Biomedical Research and Innovation.

REFERENCES

1. **Abe, T., Y. Kaname, I. Hamamoto, Y. Tsuda, X. Wen, S. Taguwa, K. Moriishi, O. Takeuchi, T. Kawai, T. Kanto, N. Hayashi, S. Akira, and Y. Matsuura.** 2007. Hepatitis C Virus nonstructural protein 5A modulates Toll-like receptor-MyD88-dependent signaling pathway in the macrophage cell lines. J. Virol. **81:**8953–8966.
2. **Aizaki, H., K. J. Lee, V. M. Sung, H. Ishiko, and M. M. Lai.** 2004. Characterization of the hepatitis C virus RNA replication complex associated with lipid rafts. Virology **324:**450–461.
3. **Behrens, S. E., L. Tomei, and R. De Francesco.** 1996. Identification and properties of the RNA-dependent RNA polymerase of hepatitis C virus. EMBO J. **15:**12–22.
4. **Blight, K. J., A. A. Kolykhalov, and C. M. Rice.** 2000. Efficient initiation of HCV RNA replication in cell culture. Science **290:**1972–1974.
5. **Egger, D., B. Wolk, R. Gosert, L. Bianchi, H. E. Blum, D. Moradpour, and K. Bienz.** 2002. Expression of hepatitis C virus proteins induces distinct membrane alterations including a candidate viral replication complex. J. Virol. **76:**5974–5984.
6. **Evans, M. J., C. M. Rice, and S. P. Goff.** 2004. Phosphorylation of hepatitis C virus nonstructural protein 5A modulates its protein interactions and viral RNA replication. Proc. Natl. Acad. Sci. USA **101:**13038–13043.
7. **Gao, L., H. Aizaki, J.-W. He, and M. M. C. Lai.** 2004. Interactions between viral nonstructural proteins and host protein hVAP-33 mediate the formation of hepatitis C virus RNA replication complex on lipid raft. J. Virol. **78:**3480–3488.
8. **Grakoui, A., D. W. McCourt, C. Wychowski, S. M. Feinstone, and C. M. Rice.** 1993. Characterization of the hepatitis C virus-encoded serine proteinase: determination of proteinase-dependent polyprotein cleavage sites. J. Virol. **67:**2832–2843.
9. **Hamamoto, I., Y. Nishimura, T. Okamoto, H. Aizaki, M. Liu, Y. Mori, T. Abe, T. Suzuki, M. M. Lai, T. Miyamura, K. Moriishi, and Y. Matsuura.** 2005. Human VAP-B is involved in hepatitis C virus replication through interaction with NS5A and NS5B. J. Virol. **79:**13473–13482.
10. **Hanada, K., K. Kumagai, S. Yasuda, Y. Miura, M. Kawano, M. Fukasawa, and M. Nishijima.** 2003. Molecular machinery for non-vesicular trafficking of ceramide. Nature **426:**803–809.
11. **Ho, S. N., H. D. Hunt, R. M. Horton, J. K. Pullen, and L. R. Pease.** 1989. Site-directed mutagenesis by overlap extension using the polymerase chain reaction. Gene **77:**51–59.
12. **Hoofnagle, J. H.** 2002. Course and outcome of hepatitis C. Hepatology **36:**S21–S29.
13. **Huang, D. C., S. Cory, and A. Strasser.** 1997. Bcl-2, Bcl-XL and adenovirus protein E1B19kD are functionally equivalent in their ability to inhibit cell death. Oncogene **14:**405–414.
14. **Ikeda, M., K. Abe, M. Yamada, H. Dansako, K. Naka, and N. Kato.** 2006. Different anti-HCV profiles of statins and their potential for combination therapy with interferon. Hepatology **44:**117–125.
15. **Inoue, K., T. Umehara, U. T. Ruegg, F. Yasui, T. Watanabe, H. Yasuda, J. M. Dumont, P. Scalfaro, M. Yoshiba, and M. Kohara.** 2007. Evaluation of a cyclophilin inhibitor in hepatitis C virus-infected chimeric mice in vivo. Hepatology **45:**921–928.
16. **Kaiser, S. E., J. H. Brickner, A. R. Reilein, T. D. Fenn, P. Walter, and A. T. Brunger.** 2005. Structural basis of FFAT motif-mediated ER targeting. Structure **13:**1035–1045.
17. **Kanekura, K., I. Nishimoto, S. Aiso, and M. Matsuoka.** 2006. Characterization of amyotrophic lateral sclerosis-linked P56S mutation of vesicle-associated membrane protein-associated protein B (VAPB/ALS8). J. Biol. Chem. **281:**30223–30233.
18. **Kapadia, S. B., and F. V. Chisari.** 2005. Hepatitis C virus RNA replication is regulated by host geranylgeranylation and fatty acids. Proc. Natl. Acad. Sci. USA **102:**2561–2566.
19. **Kawano, M., K. Kumagai, M. Nishijima, and K. Hanada.** 2006. Efficient trafficking of ceramide from the endoplasmic reticulum to the Golgi apparatus requires a VAMP-associated protein-interacting FFAT motif of CERT. J. Biol. Chem. **281:**30279–30288.
20. **Loewen, C. J., A. Roy, and T. P. Levine.** 2003. A conserved ER targeting motif in three families of lipid binding proteins and in Opi1p binds VAP. EMBO J. **22:**2025–2035.
21. **Lohmann, V., F. Korner, J. Koch, U. Herian, L. Theilmann, and R. Bartenschlager.** 1999. Replication of subgenomic hepatitis C virus RNAs in a hepatoma cell line. Science **285:**110–113.
22. **Lotz, G. P., A. Brychzy, S. Heinz, and W. M. Obermann.** 2008. A novel HSP90 chaperone complex regulates intracellular vesicle transport. J. Cell Sci. **121:**717–723.
23. **McLauchlan, J., M. K. Lemberg, G. Hope, and B. Martoglio.** 2002. Intramembrane proteolysis promotes trafficking of hepatitis C virus core protein to lipid droplets. EMBO J. **21:**3980–3988.
24. **Miyanari, Y., M. Hijikata, M. Yamaji, M. Hosaka, H. Takahashi, and K. Shimotohno.** 2003. Hepatitis C virus non-structural proteins in the probable membranous compartment function in viral genome replication. J. Biol. Chem. **278:**50301–50308.
25. **Moriishi, K., and Y. Matsuura.** 2007. Host factors involved in the replication of hepatitis C virus. Rev. Med. Virol. **17:**343–354.
26. **Moriishi, K., and Y. Matsuura.** 2003. Mechanisms of hepatitis C virus infection. Antivir. Chem. Chemother. **14:**285–297.
27. **Moriishi, K., T. Okabayashi, K. Nakai, K. Moriya, K. Koike, S. Murata, T. Chiba, K. Tanaka, R. Suzuki, T. Suzuki, T. Miyamura, and Y. Matsuura.** 2003. Proteasome activator PA28gamma-dependent nuclear retention and degradation of hepatitis C virus core protein. J. Virol. **77:**10237–10249.
28. **Nakagawa, S., T. Umehara, C. Matsuda, S. Kuge, M. Sudoh, and M. Kohara.** 2007. Hsp90 inhibitors suppress HCV replication in replicon cells and humanized liver mice. Biochem. Biophys. Res. Commun. **353:**882–888.
29. **Nishimura, A. L., M. Mitne-Neto, H. C. Silva, A. Richieri-Costa, S. Middleton, D. Cascio, F. Kok, J. R. Oliveira, T. Gillingwater, J. Webb, P. Skehel, and M. Zatz.** 2004. A mutation in the vesicle-trafficking protein VAPB causes late-onset spinal muscular atrophy and amyotrophic lateral sclerosis. Am. J. Hum. Genet. **75:**822–831.
30. **Nishimura, Y., M. Hayashi, H. Inada, and T. Tanaka.** 1999. Molecular cloning and characterization of mammalian homologues of vesicle-associated membrane protein-associated (VAMP-associated) proteins. Biochem. Biophys. Res. Commun. **254:**21–26.
31. **Niwa, H., K. Yamamura, and J. Miyazaki.** 1991. Efficient selection for high-expression transfectants with a novel eukaryotic vector. Gene **108:**193–199.
32. **Okamoto, K., Y. Mori, Y. Komoda, T. Okamoto, M. Okochi, M. Takeda, T. Suzuki, K. Moriishi, and Y. Matsuura.** 2008. Intramembrane processing by signal peptide peptidase regulates the membrane localization of hepatitis C virus core protein and viral propagation. J. Virol. **82:**8349–8361.
33. **Okamoto, K., K. Moriishi, T. Miyamura, and Y. Matsuura.** 2004. Intramembrane proteolysis and endoplasmic reticulum retention of hepatitis C virus core protein. J. Virol. **78:**6370–6380.
34. **Okamoto, T., Y. Nishimura, T. Ichimura, K. Suzuki, T. Miyamura, T. Suzuki, K. Moriishi, and Y. Matsuura.** 2006. Hepatitis C virus RNA replication is regulated by FKBP8 and Hsp90. EMBO J. **25:**5015–5025.
35. **Okamoto, T., H. Omori, Y. Kaname, T. Abe, Y. Nishimura, T. Suzuki, T. Miyamura, T. Yoshimori, K. Moriishi, and Y. Matsuura.** 2008. A single-amino-acid mutation in hepatitis C virus NS5A disrupting FKBP8 interaction impairs viral replication. J. Virol. **82:**3480–3489.
36. **Pennetta, G., P. R. Hiesinger, R. Fabian-Fine, I. A. Meinertzhagen, and H. J. Bellen.** 2002. Drosophila VAP-33A directs bouton formation at neuromuscular junctions in a dosage-dependent manner. Neuron **35:**291–306.
37. **Prosser, D. C., D. Tran, P. Y. Gougeon, C. Verly, and J. K. Ngsee.** 2008. FFAT rescues VAPA-mediated inhibition of ER-to-Golgi transport and VAPB-mediated ER aggregation. J. Cell Sci. **121:**3052–3061.
38. **Skehel, P. A., R. Fabian-Fine, and E. R. Kandel.** 2000. Mouse VAP33 is associated with the endoplasmic reticulum and microtubules. Proc. Natl. Acad. Sci. USA **97:**1101–1106.
39. **Skehel, P. A., K. C. Martin, E. R. Kandel, and D. Bartsch.** 1995. A VAMP-binding protein from *Aplysia* required for neurotransmitter release. Science **269:**1580–1583.
40. **Taguwa, S., T. Okamoto, T. Abe, Y. Mori, T. Suzuki, K. Moriishi, and Y. Matsuura.** 2008. Human butyrate-induced transcript 1 interacts with hepatitis C virus NS5A and regulates viral replication. J. Virol. **82:**2631–2641.
41. **Tellinghuisen, T. L., J. Marcotrigiano, and C. M. Rice.** 2005. Structure of the zinc-binding domain of an essential component of the hepatitis C virus replicase. Nature **435:**374–379.
42. **Tomei, L., C. Failla, E. Santolini, R. De Francesco, and N. La Monica.** 1993. NS3 is a serine protease required for processing of hepatitis C virus polyprotein. J. Virol. **67:**4017–4026.
43. **Tsuda, H., S. M. Han, Y. Yang, C. Tong, Y. Q. Lin, K. Mohan, C. Haueter, A. Zoghbi, Y. Harati, J. Kwan, M. A. Miller, and H. J. Bellen.** 2008. The amyotrophic lateral sclerosis 8 protein VAPB is cleaved, secreted, and acts as a ligand for Eph receptors. Cell **133:**963–977.
44. **Tu, H., L. Gao, S. T. Shi, D. R. Taylor, T. Yang, A. K. Mircheff, Y. Wen, A. E. Gorbalenya, S. B. Hwang, and M. M. Lai.** 1999. Hepatitis C virus RNA polymerase and NS5A complex with a SNARE-like protein. Virology **263:**30–41.

45. **Ujino, S., S. Yamaguchi, K. Shimotohno, and H. Takaku.** 2009. Heat-shock protein 90 is essential for stabilization of the hepatitis C virus non-structural protein NS3. J. Biol. Chem. **284:**6841–6846.
46. **Wang, C., M. Gale, Jr., B. C. Keller, H. Huang, M. S. Brown, J. L. Goldstein, and J. Ye.** 2005. Identification of FBL2 as a geranylgeranylated cellular protein required for hepatitis C virus RNA replication. Mol. Cell **18:**425–434.
47. **Wasley, A., and M. J. Alter.** 2000. Epidemiology of hepatitis C: geographic differences and temporal trends. Semin. Liver Dis. **20:**1–16.
48. **Watashi, K., N. Ishii, M. Hijikata, D. Inoue, T. Murata, Y. Miyanari, and K. Shimotohno.** 2005. Cyclophilin B is a functional regulator of hepatitis C virus RNA polymerase. Mol. Cell **19:**111–122.
49. **Weir, M. L., A. Klip, and W. S. Trimble.** 1998. Identification of a human homologue of the vesicle-associated membrane protein (VAMP)-associated protein of 33 kDa (VAP-33): a broadly expressed protein that binds to VAMP. Biochem. J. **333:**247–251.
50. **Weir, M. L., H. Xie, A. Klip, and W. S. Trimble.** 2001. VAP-A binds promiscuously to both v- and tSNAREs. Biochem. Biophys. Res. Commun. **286:**616–621.
51. **Zhong, J., P. Gastaminza, G. Cheng, S. Kapadia, T. Kato, D. R. Burton, S. F. Wieland, S. L. Uprichard, T. Wakita, and F. V. Chisari.** 2005. Robust hepatitis C virus infection in vitro. Proc. Natl. Acad. Sci. USA **102:**9294–9299.

Virus Research 163 (2012) 405–409

Contents lists available at SciVerse ScienceDirect

Virus Research

journal homepage: www.elsevier.com/locate/virusres

Short communication

Translocase of outer mitochondrial membrane 70 induces interferon response and is impaired by hepatitis C virus NS3

Yuri Kasama[a], Makoto Saito[a], Takashi Takano[b], Tomohiro Nishimura[c], Masaaki Satoh[a,d], Zhongzhi Wang[a], Salem Nagla Elwy Salem Ali[a,e], Shinji Harada[e], Michinori Kohara[f], Kyoko Tsukiyama-Kohara[a,*]

[a] Department of Experimental Phylaxiology, Faculty of Life Sciences, Kumamoto University, 1-1-1 Honjo Kumamoto City, Kumamoto 860-8556, Japan
[b] Division of Veterinary Public Health, Nippon Veterinary and Life Science University, 1-7-1 Kyonan, Musashino, Tokyo 180-8602, Japan
[c] KAKETSUKEN, Kyokushi, Kikuchi, Kumamoto 869-1298, Japan
[d] Department of Virology I, National Institute of Infectious Diseases, Tokyo 162-8640, Japan
[e] Department of Medical Virology, Faculty of Life Sciences, Kumamoto University, Japan
[f] Department of Microbiology and Cell Biology, Tokyo Metropolitan Institute of Medical Science, 2-1-6 Kamikitazawa, Setagaya-ku, Tokyo 156-8506, Japan

ARTICLE INFO

Article history:
Received 5 September 2011
Received in revised form 13 October 2011
Accepted 13 October 2011
Available online 20 October 2011

Keywords:
HCV
Tom70
MAVS
IFN
IRF-3
NS3

ABSTRACT

Hepatitis C virus (HCV) elevated expression of the translocase of outer mitochondrial membrane 70 (Tom70). Interestingly, overexpression of Tom70 induces interferon (IFN) synthesis in hepatocytes, and it was impaired by HCV. Here, we addressed the mechanism of this impairment. The HCV NS3/4A protein induced Tom70 expression. The HCV NS3 protein interacted in cells, and cleaved the adapter protein mitochondrial anti-viral signaling (MAVS). Ectopic overexpression of Tom70 could not inhibit this cleavage. As a result, IRF-3 phosphorylation was impaired and IFN-β induction was suppressed. These results indicate that MAVS works upstream of Tom70 and the cleavage of MAVS by HCV NS3 protease suppresses signaling of IFN induction.

Type I interferon (IFN) induction is the front line of host defense against viral infection. Intracellular double-stranded RNA is a viral replication intermediate and contains pathogen-associated molecular patterns (PAMPS) (Saito et al., 2008) that are recognized by pathogen-recognition receptors (PRRs) to induce IFN. One PRR family includes the Toll-like receptors (TLRs), which are predominantly expressed in the endosome (Heil et al., 2004). Another route of IFN induction takes place in the cytosol through activation of specific RNA helicases, such as retinoic acid-inducible (RIG)-I and melanoma differentiation associated gene 5 (MDA5). The ligand for RIG-I is an uncapped 5′ triphosphate RNA, which is found in viral RNAs of the *Flaviviridae* family, including hepatitis C virus (HCV), paramyxovirus, and rhabdoviruses (Kato et al., 2006). MDA5 recognizes viruses with protected 5′ RNA ends, for example, picornaviruses (Hornung et al., 2006). The adapter protein that links the RNA helicase to the downstream MAPK, NF-κB, and IRF-3 signaling pathways is referred to as the mitochondrial anti-viral signaling (MAVS) protein (Seth et al., 2005); alternative names include IPS-1, interferon-promoter stimulator 1; VISA, virus-induced signaling adaptor; and CARDIF, CARD adapter inducing IFN. HCV nonstructural protein 3 (NS3) possesses a serine protease domain at the N terminus (amino acids (aa) 1–180) and has been found to cleave adaptor proteins, MAVS at aa 508 (Meylan et al., 2005) and Toll/IL-1R domain-containing adapter inducing IFN-β-deficient (TRIF at aa 372; Ferreon et al., 2005). These cleavages provoke abrogation of the induction of the IFN pathway.

The translocase of the outer membrane (TOM) is responsible for initial recognition of mitochondrial preproteins in the cytosol (Baker et al., 2007; Neupert and Herrmann, 2007). The TOM machinery consists of 2 import receptors, Tom20 and Tom70, and, along with several other subunits, comprises the general import pore (Abe et al., 2000). Recently, Tom70 was found to interact with MAVS (Liu et al., 2010). Ectopic expression or silencing of Tom70, respectively, enhanced or impaired IRF3-mediated gene expression and IFN-β production. Sendai virus infection accelerated the

* Corresponding author. Present address: Transboundary Animal Diseases Center, Faculty of Agriculture, Kagoshima University, 1-21-24 Korimoto Kagoshima-shi, Kagoshima 890-0065, Japan. Tel.: +81 99 285 3589/96 373 5560; fax: +81 99 285 3589/96 373 5562.
E-mail address: kkohara@kumamoto-u.ac.jp (K. Tsukiyama-Kohara).

0168-1702/$ – see front matter © 2011 Elsevier B.V. All rights reserved.
doi:10.1016/j.virusres.2011.10.009

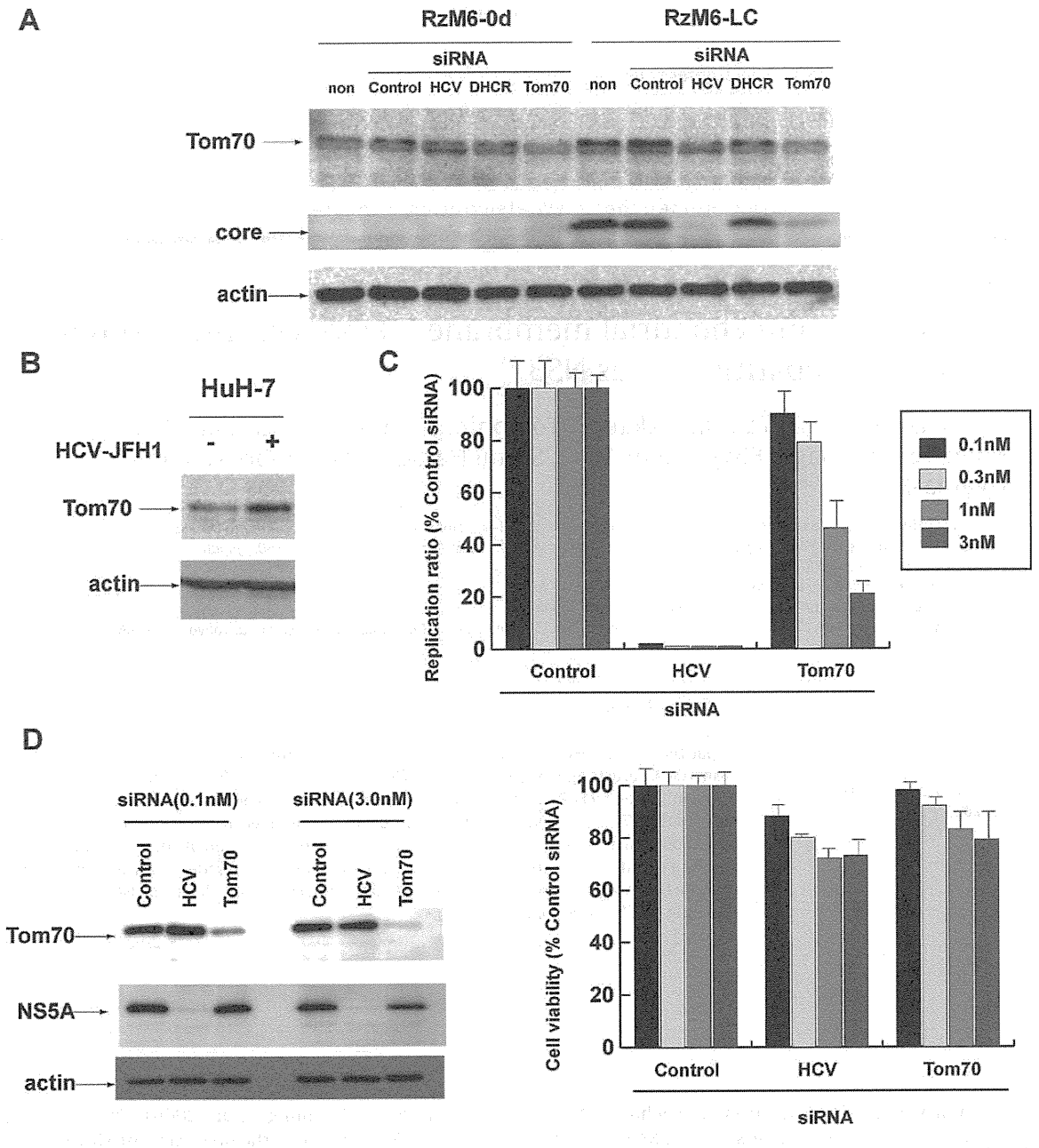

Fig. 1. HCV induces overexpression of Tom70 but impairs Tom70-induced IFN synthesis. (A) RzM6 cells (HCV-) and RzM6-LC cells (HCV+) were transfected with siRNAs of control (non-target siRNA#3: Thermo Fisher Scientific), HCV (R5: 5′-GUCUCGUAGACCGUGCAUCAuu-3′), DHCR24 (Nishimura et al., 2009), and Tom70 (Takano et al., 2011a). Control cells were mock-transfected. Tom70 protein was detected with MAb2-243a (Takano et al., 2011a) and actin protein was detected as an internal control (lower column). (B) HuH-7 cells were infected with HCV JFH-1 strain; Tom70 protein and actin protein were detected. (C) The HCV replicon cells (FLR3-1; Takano et al., 2011b) were transfected with siRNAs (control, HCV (R7: 5′-GUCUCGUAGACCGUGCACCAuu-3′), Tom70; 0.1, 0.3, 1, 3 nM) and HCV replication activity was measured with luciferase activity using the Bright-Glo luciferase assay kit (Promega). Cell viability was measured using WST-8 (Dojindo) reagent. Ratio with those of control siRNA treatment was calculated. Vertical bars were S.D. (D) HCV replicon cells (FLR3-1) were transfected with control, HCV (R7) and Tom70 siRNAs (0.1, 0.3 nM) and Tom70, NS5A and actin proteins were detected.

Tom70-mediated IFN induction and the interaction of Tom70 with MAVS. These recent findings indicated that Tom70 might be a critical mediator during IFN induction (Liu et al., 2010).

We previously observed that HCV induces Tom70 and is related to the apoptotic response (Takano et al., 2011a). However, no synergistic effect was observed for IFN induction by Tom70 and HCV. Therefore, in the present study, we have investigated the mechanism of modification of the Tom70-induced IFN synthesis pathway by HCV and clarified a finely balanced system regulated by viral protein.

The expression of Tom70 protein was examined using western blotting and modification by HCV was characterized (Fig. 1A). The level of Tom70 protein was increased in RzM6-LC cells compared with that in RzM6-0d cells (Tsukiyama-Kohara et al., 2004). The full-length HCV-RNA expression was induced by 4-hydroxytamoxifen (100 nM) and passaged for more than 44 days in RzM6-LC cells, and HCV expression was not induced in RzM6-0d cells. Silencing of HCV expression by siRNA (R5; Thermo Scientific) abolished core protein expression, and decreased the level of Tom70 protein expression in RzM6-LC cells (Fig. 1A). Silencing of Tom70 by siRNA significantly decreased the level of HCV core protein expression in RzM6-LC cells (Fig. 1A). The siRNA against 3-beta-hydroxysterol-delta24 reductase (DHCR24) slightly decreased the level of Tom70 protein. In contrast, the

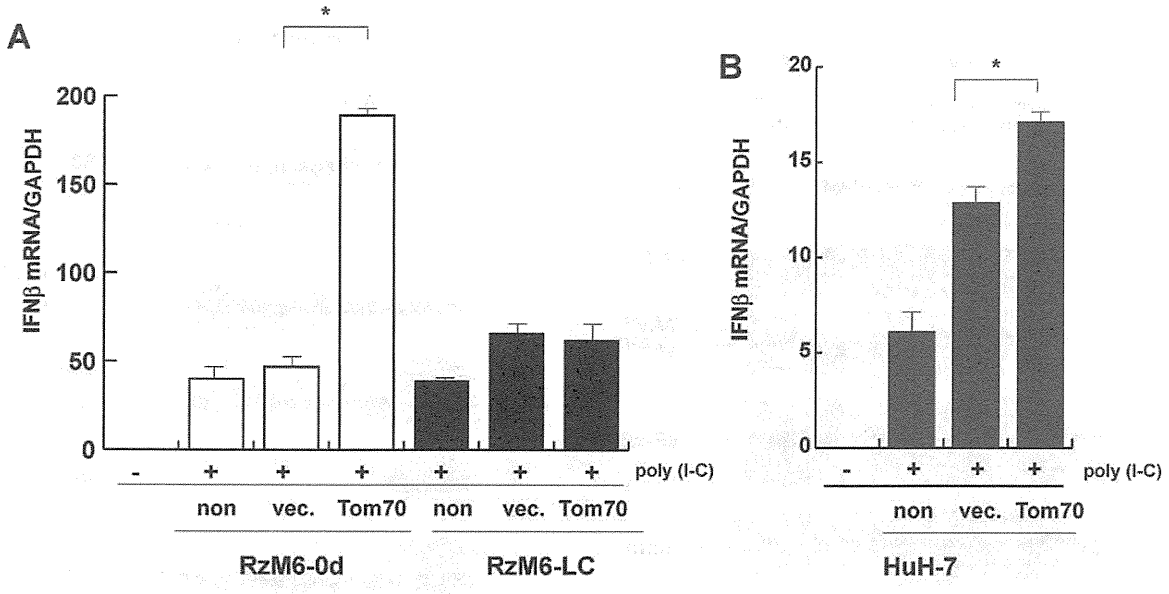

Fig. 2. Tom70-induced IFN synthesis was impaired by HCV. (A) RzM6-0d cells and LC cells were transfected with mock-vector, control pcDNA vector (vec.), or pcDNA-Tom70 expression vector, and the amount of IFN-β mRNA was measured by RTD-PCR and normalized to the amount of GAPDH mRNA using Gene expression assay kit (GE-Healthcare). Poly(I–C) (GE Healthcare) (5 μg) was transfected with RNAi Max reagent (Invitrogen) and IFN-βmRNA was measured after 6 h of poly(I–C) treatment. Vertical bars indicate S.D. $^*p < 0.05$. (B) HuH-7 cells were transfected with mock-vector, control vector, or Tom70 expression vector, and the amount of IFN-β mRNA was measured by RTD-PCR and normalized to the amount of GAPDH mRNA. Vertical bars indicate S.D. $^*p < 0.05$.

control siRNA did not have a significant effect on Tom70 protein expression.

We next examined the effects of HCV JFH-1 (Wakita et al., 2005) infection on Tom70 expression (Fig. 1B). Infection with HCV significantly increased the level of Tom70 protein expression. We also examine the role of Tom70 in HCV replication (Fig. 1C and D). Silencing of Tom70 by siRNA decreased the HCV replication in a dose dependent manner.

Thus, HCV induces Tom70 expression, and Tom70 is involved in viral replication.

It was recently shown that Tom70 recruits TBK1/IRF3 to mitochondria by binding to Hsp90 and inducing IFN-β synthesis (Liu et al., 2010). Therefore, we examined the effects of Tom70 overexpression on IFN synthesis and modification by HCV (Fig. 2). Level of IFN-β mRNA synthesis was quantitated by real-time detection (RTD) PCR. Overexpression of Tom70 by transfection of pcDNA6-Tom70 (Takano et al., 2011a) induced IFN-β mRNA synthesis in the absence of HCV after poly(I–C) treatment (RzM6-0d cells). However, the Tom70-mediated induction of IFN-β mRNA transcription was impaired in the presence of HCV (RzM6-LC cells) (Fig. 2A). Overexpression of Tom70 induced IFN-β mRNA synthesis in HuH-7 cells (Fig. 2B). Induction of IFN-β mRNA was lower in HuH-7 cells than HepG2 based RzM6 cells, which might be due to the defect in IFN induction system in HuH-7 cells (Preiss et al., 2008).

We have further addressed the mechanism of impairment of IFN-β mRNA transcription by HCV.

To identify the viral protein that was responsible for the induction of Tom70, we examined the Tom70 protein expression levels in HCV core, E1, E2, NS2, NS3/4A, NS4B, NS5A, and NS5B protein-expressing cells (data not shown), and Tom70 protein expression level was highest in the NS3/4A-expressing cells than was observed in cells expressing other proteins (Fig. 3A, data not shown), indicating an effect of HCV NS3/4A protein on Tom70 expression.

The expression vector of Myc- and His-tagged Tom70 was transfected into the empty control or NS3/4A-expressing cells and immunoprecipitated with anti-Myc antibody (Suppl. Fig. 1A). Results showed that Myc-Tom70 was precipitated in both cells (right panel) and NS3 protein was specifically precipitated by anti-Myc antibody in the NS3/4A-expressing cells (left panel). NS4A protein could not be detected (data not shown).

We next stained the NS3/4A-expressing cells with anti-NS3 and -Tom70 antibodies, and observed with confocal microscopy (Suppl. Fig. 1B). The signal of NS3 protein was clearly merged with that of Tom70, strongly supporting the possibility that the NS3 protein co-localizes with the Tom70 protein.

To clarify the effect of Tom70 on NS3, we transfected NS3/4A-expressing cells with the siRNA of Tom70 (Fig. 3A). Silencing of Tom70 decreased the level of NS3 protein in cells, but did not influence the levels of the MAVS and NF-κB proteins. These results suggest the possibility that Tom70 may increase the stability of NS3 protein in cells.

Tom70 reportedly interacts with MAVS during viral infection (Liu et al., 2010). Therefore, we examined the MAVS protein in cells expressing either the control empty or NS3/4A lenti-virus vector (Fig. 3B). Cleavage of MAVS (indicated as ΔMAVS) was observed in NS3/4A protein-expressing cells, as was reported previously (Meylan et al., 2005). Overexpression of Tom70 did not have a significant effect on the MAVS expression level and did not prevent MAVS cleavage by NS3. IRF-3 phosphorylation was suppressed in NS3/4A-expressing cells and was not influenced by Tom70 overexpression. The induction of IFN-β was impaired in NS3/4A-expressing cells, even in the presence of Tom70 overexpression (Fig. 3C). These data may indicate that MAVS exists upstream of Tom70 and that cleavage of MAVS by NS3/4A impaired the downstream signaling activation of IRF-3 phosphorylation (Suppl. Fig. 2).

Mitochondria provide a substantial platform for the regulation of IFN signaling. The MAVS adapter protein is a member of the family of RIG-I like receptors (RLRs), which links the mitochondria to the mammalian antiviral defense system (Seth et al., 2005). Proteomic studies have demonstrated that MAVS interacts with Tom70 (Liu et al., 2010). This interaction was accelerated by Sendai virus infection and synergized with ectopic expression of Tom70 to significantly increase the production of IFN-β (Liu et al., 2010). The results of the present study revealed that infection with HCV induced Tom70 expression, but the presence of HCV impaired IFN

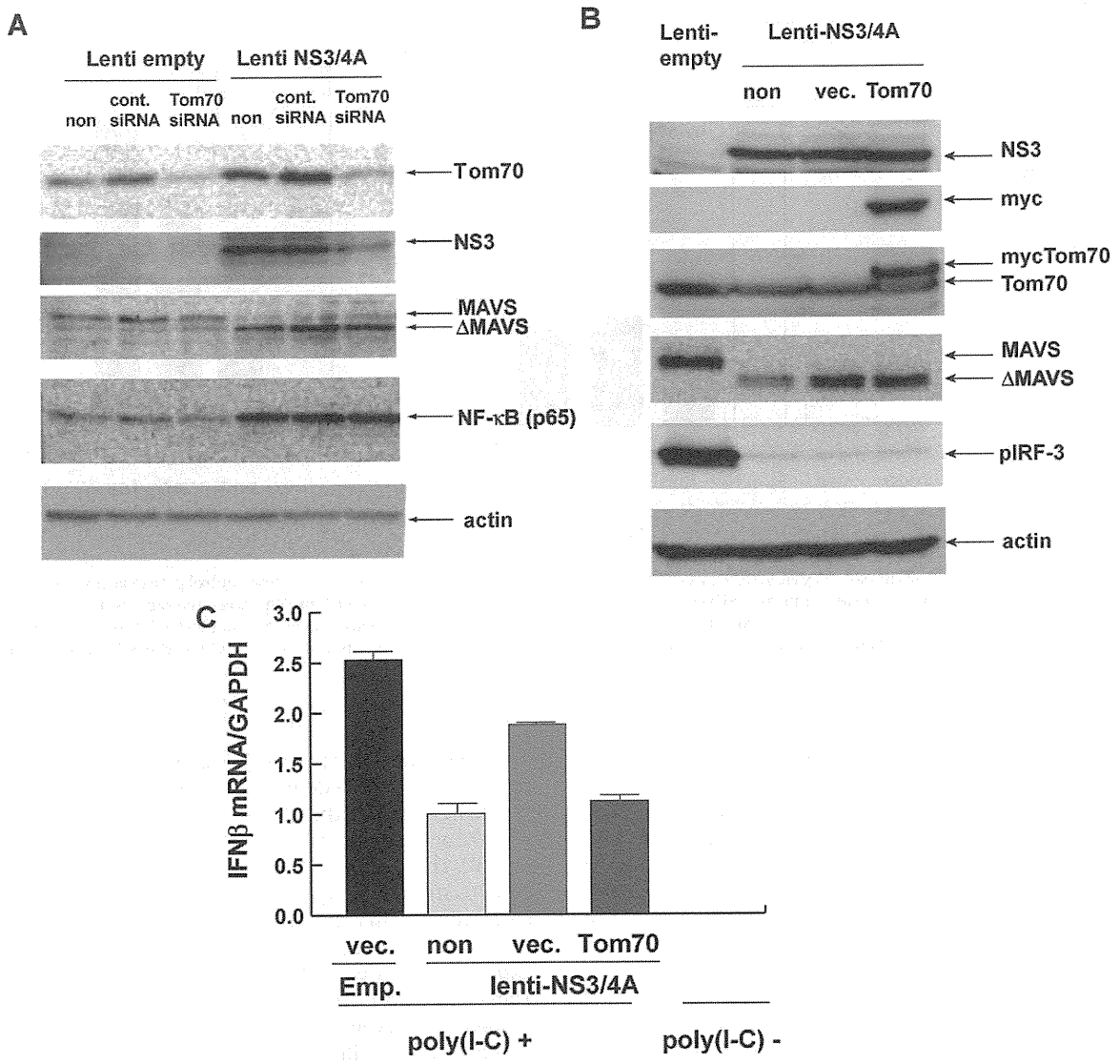

Fig. 3. Silencing of Tom70 decreased the level of NS3 and cleavage of MAVS by NS3/4A impaired IRF-3 phosphorylation even in the presence of Tom70. (A) Empty or NS3/4A-lenti virus vector expressing HepG2 cells were transfected with control siRNA and Tom70 siRNA or mock-transfected (non) as a control. MAVS, NS3, Tom70, and actin proteins were detected by western blot. (B) Empty or NS3/4A-expressing HepG2 cells were transfected with control pcDNA vector (vec.) and pcDNA6 (Invitrogen)-Tom70 or mock-transfected (non) as a control. NS3, Tom70, phosphorylated IRF-3, MAVS, and actin proteins were examined by western blot. (C) IFN-β mRNA was measured by RTD-PCR and normalized with GAPDH mRNA amount in empty or NS3/4A expressing cells with transfection of mock (non), pcDNA-vector (vec.) or pcDNA-Tom70 (Tom70). Poly(I–C) was treated, as described in the legend of Fig. 2.

induction. It has been reported that the C-terminal transmembrane domain (TM) of MAVS interacts with the N-terminal transmembrane domain of Tom70 (Liu et al., 2010). The HCV NS3 protein cleaves MAVS at residue 508 (Meylan et al., 2005), which should impair the interaction of MAVS and Tom70. This may attenuate the downstream signaling pathway (TBK-IRF3) and the induction of IFN synthesis (Suppl. Fig. 2). In our study, the level of NF-κB protein was not significantly influenced by Tom70 in the presence or absence of NS3. This may indicate that other pathways, such as TLR3 and downstream pathways, might compensate to maintain the NF-κB protein expression level in the absence of the MAVS-Tom70 signaling pathway.

Infection with HCV induced expression of Tom70, but the activation of the IFN signaling pathway was abrogated by the HCV NS3 protease. These findings indicate that recovery of the MAVS-Tom70 pathway may be a means to increase the efficacy of IFN therapy against HCV infection.

Recently, we observed that overexpression of Tom70 increased the resistance to the TNFα-induced apoptotic response (Takano et al., 2011a), indicating that Tom70 overexpression might contribute to the apoptotic resistance of HCV-infected cells and the establishment of persistent HCV infection. Thus, Tom70 might be a novel target for the regulation of HCV infection.

Acknowledgements

Authors thank Professor Yoshiharu Matsuura for providing the rabbit polyclonal NS5A antibody. This work was supported by grants from the Ministry of Health, Labor, and Welfare of Japan and the Ministry of Education, Culture, Sports, Science, and Technology of Japan.

Appendix A. Supplementary data

Supplementary data associated with this article can be found, in the online version, at doi:10.1016/j.virusres.2011.10.009.

References

Abe, Y., Shodai, T., Muto, T., Mihara, K., Torii, H., Nishikawa, S., Endo, T., Kohda, D., 2000. Structural basis of presequence recognition by the mitochondrial protein import receptor Tom20. Cell 100 (5), 551–560.

Baker, M.J., Frazier, A.E., Gulbis, J.M., Ryan, M.T., 2007. Mitochondrial protein-import machinery: correlating structure with function. Trends Cell Biol. 17 (9), 456–464.

Ferreon, J.C., Ferreon, A.C., Li, K., Lemon, S.M., 2005. Molecular determinants of TRIF proteolysis mediated by the hepatitis C virus NS3/4A protease. J. Biol. Chem. 280 (21), 20483–20492.

Heil, F., Hemmi, H., Hochrein, H., Ampenberger, F., Kirschning, C., Akira, S., Lipford, G., Wagner, H., Bauer, S., 2004. Species-specific recognition of single-stranded RNA via toll-like receptor 7 and 8. Science 303 (5663), 1526–1529.

Hornung, V., Ellegast, J., Kim, S., Brzozka, K., Jung, A., Kato, H., Poeck, H., Akira, S., Conzelmann, K.K., Schlee, M., Endres, S., Hartmann, G., 2006. 5′-Triphosphate RNA is the ligand for RIG-I. Science 314 (5801), 994–997.

Kato, H., Takeuchi, O., Sato, S., Yoneyama, M., Yamamoto, M., Matsui, K., Uematsu, S., Jung, A., Kawai, T., Ishii, K.J., Yamaguchi, O., Otsu, K., Tsujimura, T., Koh, C.S., Reis e Sousa, C., Matsuura, Y., Fujita, T., Akira, S., 2006. Differential roles of MDA5 and RIG-I helicases in the recognition of RNA viruses. Nature 441 (7089), 101–105.

Liu, X.Y., Wei, B., Shi, H.X., Shan, Y.F., Wang, C., 2010. Tom70 mediates activation of interferon regulatory factor 3 on mitochondria. Cell Res. 20 (9), 994–1011.

Meylan, E., Curran, J., Hofmann, K., Moradpour, D., Binder, M., Bartenschlager, R., Tschopp, J., 2005. Cardif is an adaptor protein in the RIG-I antiviral pathway and is targeted by hepatitis C virus. Nature 437 (7062), 1167–1172.

Neupert, W., Herrmann, J.M., 2007. Translocation of proteins into mitochondria. Annu. Rev. Biochem. 76, 723–749.

Nishimura, T., Kohara, M., Izumi, K., Kasama, Y., Hirata, Y., Huang, Y., Shuda, M., Mukaidani, C., Takano, T., Tokunaga, Y., Nuriya, H., Satoh, M., Saito, M., Kai, C., Tsukiyama-Kohara, K., 2009. Hepatitis C virus impairs p53 via persistent overexpression of 3beta-hydroxysterol Delta24-reductase. J. Biol. Chem. 284 (52), 36442–36452.

Preiss, S., Thompson, A., Chen, X., Rodgers, S., Markovska, V., Desmond, P., Visvanathan, K., Li, K., Locarnini, S., Revill, P., 2008. Characterization of the innate immune signalling pathways in hepatocyte cell lines. J. Viral Hepat. 15 (12), 888–900.

Saito, T., Owen, D.M., Jiang, F., Marcotrigiano, J., Gale Jr., M., 2008. Innate immunity induced by composition-dependent RIG-I recognition of hepatitis C virus RNA. Nature 454 (7203), 523–527.

Seth, R.B., Sun, L., Ea, C.K., Chen, Z.J., 2005. Identification and characterization of MAVS, a mitochondrial antiviral signaling protein that activates NF-kappaB and IRF 3. Cell 122 (5), 669–682.

Takano, T., Kohara, M., Kasama, Y., Nishimura, T., Saito, M., Kai, C., Tsukiyama-Kohara, K., 2011a. Translocase of outer mitochondrial membrane 70 expression is induced by hepatitis C virus and is related to the apoptotic response. J. Med. Virol. 83 (5), 801–809.

Takano, T., Tsukiyama-Kohara, K., Hayashi, M., Hirata, Y., Satoh, M., Tokunaga, Y., Tateno, C., Hayashi, Y., Hishima, T., Funata, N., Sudo, M., Kohara, M., 2011b. Augmentation of DHCR24 expression by hepatitis C virus infection facilitates viral replication in hepatocytes. J. Hepatol. 55 (3), 512–521.

Tsukiyama-Kohara, K., Tone, S., Maruyama, I., Inoue, K., Katsume, A., Nuriya, H., Ohmori, H., Ohkawa, J., Taira, K., Hoshikawa, Y., Shibasaki, F., Reth, M., Minatogawa, Y., Kohara, M., 2004. Activation of the CKI-CDK-Rb-E2F pathway in full genome hepatitis C virus-expressing cells. J. Biol. Chem. 279 (15), 14531–14541.

Wakita, T., Pietschmann, T., Kato, T., Date, T., Miyamoto, M., Zhao, Z., Murthy, K., Habermann, A., Krausslich, H.G., Mizokami, M., Bartenschlager, R., Liang, T.J., 2005. Production of infectious hepatitis C virus in tissue culture from a cloned viral genome. Nat. Med. 11 (7), 791–796.

MAJOR ARTICLE

Monoclonal Antibody 2-152a Suppresses Hepatitis C Virus Infection Through Betaine/GABA Transporter-1

Masaaki Satoh,[1] Makoto Saito,[1] Takashi Takano,[1,2] Yuri Kasama,[1] Tomohiro Nishimura,[1,3] Yasumasa Nishito,[4] Yuichi Hirata,[2] Masaaki Arai,[2] Masayuki Sudoh,[5] Chieko Kai,[6] Michinori Kohara,[2] and Kyoko Tsukiyama-Kohara[1]

[1]Department of Experimental Phylaxiology, Faculty of Life Sciences, Kumamoto University, Honjo Kumamoto City; [2]Department of Microbiology and Cell Biology, Tokyo Metropolitan Institute of Medical Science, Kamikitazawa, Setagaya-ku; [3]KAKETSUKEN, Kyokushi, Kikuchi, Kumamoto; [4]Center for Microarray Analysis, Tokyo Metropolitan Institute of Medical Science; [5]Kamakura Research Laboratories, Chugai Pharmaceutical Co., Ltd., Kajiwara, Kamakura-City, Kanagawa; and [6]Laboratory of Animal Research Center, Institute of Medical Science, University of Tokyo, Shirokane-dai Minato-Ku, Japan

Background. We recently established a monoclonal antibody (2-152a MAb) that binds to 3β-hydroxysterol-Δ24-reductase (DHCR24) by immunizing mice with cells (RzM6-LC) persistently expressing hepatitis C virus (HCV). Here, we aimed to analyze the activity of 2-152a MAb against HCV replication and explore the molecular mechanism underlying the antiviral activity.

Methods. We characterized the effects of 2-152a MAb on HCV replication and performed a microarray analysis of antibody-treated HCV replicon cells. The molecules showing a significant change after the antibody treatment were screened to examine their relationship with HCV replication.

Results. The antibody had antiviral activity both in vitro and in vivo (chimeric mice). In the microarray analysis, 2-152a MAb significantly suppressed the expression of betaine/GABA transporter-1 (BGT-1) in 2 HCV replicon cell lines but not in HCV-cured cells. Silencing of BGT-1 expression by small interfering RNA (siRNA) revealed significant suppression of HCV replication and infection without cytotoxicity. Further, BGT-1 expression was significantly increased in the presence of HCV ($P < .05$).

Conclusions. Our results suggest that 2-152a MAb suppresses HCV replication and infection through BGT-1. These findings highlight important roles of BGT-1 in HCV replication and reveal a possible target for anti-HCV therapy.

Hepatitis C virus (HCV) causes chronic hepatitis and hepatocellular carcinoma (HCC) [1–3]. Chronic HCV infection is a major global public health concern because it affects at least 170 million people worldwide [2]. The most effective treatment against HCV currently comprises a combination therapy of PEGylated α-interferon (IFN-α) and ribavirin [4, 5]. However, considering that sustained virological responses develop in only approximately half of the patients infected with HCV genotype 1, the clinical efficacy of this therapy is limited [6, 7]. Efforts to develop therapies against HCV are further hindered by the high level of viral variation and capacity of the virus to cause chronic infection. Therefore, there is an urgent need to develop effective treatments against chronic HCV infection.

In a previous study, we established a cell line expressing HCV (RzM6-LC) to investigate the effects of persistent HCV expression on cell growth [8]. We also established a monoclonal antibody (2-152a MAb) against the RzM6-LC cell line to produce clones that recognize both cell surface and intracellular molecules. Using this method, we identified 3b-hydroxysterol-D24-reductase (DHCR24) as the recognition molecule of this antibody.

Received 30 November 2010; accepted 10 May 2011.

Correspondence: Kyoko Tsukiyama-Kohara, PhD, DVM, Department of Experimental Phylaxiology, Faculty of Life Sciences, Kumamoto University, 1-1-1 Honjo, Kumamoto-shi, Kumamoto 860-8556, Japan (kkohara@kumamoto-u.ac.jp).

The Journal of Infectious Diseases 2011;204:1172–80

0022-1899 (print)/1537-6613 (online)/2011/2048-0005$14.00
DOI: 10.1093/infdis/jir501

DHCR24 (also termed seladin-1) is an enzyme that catalyzes the conversion of desmosterol to cholesterol in the postsqualene cholesterol biosynthetic pathway [9, 10]. DHCR24 also acts as a hydrogen peroxide scavenger [11]. Therefore, DHCR24 may play a crucial role in maintaining cell physiology through cholesterol synthesis and oxidative stress. We previously demonstrated that HCV infection upregulates DHCR24 expression, and overexpression of DHCR24 inhibits apoptosis and inactivates the tumor suppressor gene p53 [12]. Moreover, silencing of DHCR24 suppressed HCV replication [13]. However, the precise mechanisms through which DHCR24 affects the HCV life cycle are unclear. In this study, we aimed to analyze the activity of 2-152a MAb against HCV replication and explore the molecular mechanism underlying the antiviral activity.

Materials And Methods

Cell Lines and Reagents

Human hepatoma cell line HuH-7 cell-based HCV replicon-harboring cell lines [14] R6FLR-N (genotype 1b) [15], FLR3-1 (genotype 1b) [16], and JFH-1 (genotype 2a) [17] were maintained in Dulbecco's modified Eagle's medium (DMEM) GlutaMAX (Invitrogen) containing 10% fetal calf serum (FCS; Sigma-Aldrich) in the presence of G418 (500 mg/mL for R6FLR-N and FLR3-1, 300 mg/mL for JFH-1; Invitrogen). Cured/HuH-7 histone H3 lysine 4 (K4) cells cured off HCV by interferon treatment [18] were maintained in DMEM GlutaMAX containing 10% FCS without G418. The JFH/K4 cell line persistently infected with the HCV JFH-1 strain and HuH-7 cell lines were maintained in DMEM containing 10% FCS [19]. The human hepatoblastoma HepG2 cell line was also maintained in DMEM containing 10% FCS.

Generation of 2-152a MAb

BALB/c strain of mice was immunized with 7–8 intraperitoneal injections of RzM6-LC cells (5×10^6) in RIBI adjuvant (trehalose dimycolate + monophosphoryl lipid A emulsion; RIBI ImmunoChem Research). After completion of the immunization regimen, their spleens were excised and splenocytes were fused with mouse myeloma plasminogen activator inhibitor (PAI) cells by using PEG1500 (Roche). Hybridoma cells were then selected with hypoxanthine, aminopterin, and thymidine (Invitrogen), and culture supernatants were collected for screening by whole-cell enzyme-linked immunosorbent assay (ELISA).

HCV Infection in Humanized Chimeric Mouse Liver and HCV mRNA Quantification by Real-time Detection Polymerase Chain Reaction

We purchased (from PhoenixBio Co.) chimeric mice that were established by transplanting human primary hepatocytes into severely combined immunodeficient (SCID) mice carrying a urokinase plasminogen activator (uPA) transgene controlled by an albumin promoter [20]. These mice were then infected with plasma isolated before 2003 from an HCV-positive patient (HCR6) [8, 21], in accordance with the Declaration of Helsinki. The protocols for the animal experiments were preapproved by the local ethics committee, and the animals were maintained in accordance with the National Institutes of Health Guide for the Care and Use of Laboratory Animals. HCV genotype 1b RNA levels were established at $0.96–1.84 \times 10^7$ copies/mL in mouse serum samples before the antibody treatment. The antibody (2-152a MAb) and normal immunoglobin G (IgG, 400 mg/20 g body weight) were intraperitoneally injected into the mice ($n = 4$) at 2-day intervals over a period of 14 days. IFN-α (30 mg/kg) was administered subcutaneously at 2-day intervals over a period of 2 weeks. Human serum albumin in the blood of chimeric mice was measured by using an Alb-II kit according to the manufacturer's instructions (Eiken Chemical). HCV RNA levels in serum and JFH/K4 cells were measured by real-time detection polymerase chain reaction (real-time detection [RTD]-PCR) as described previously [22]. HCV RNA in the cell cultures and supernatants was extracted by using Isogene and Isogene LS (Nippon Gene), respectively.

Replication Assay Using HCV Replicon Cells

We used 3 HCV subgenomic replicon cell lines: R6FLR-N, FLR3-1, and JFH-1. They were seeded at a density of 5×10^3 cells/well in 96-well tissue culture plates in DMEM GlutaMAX (Invitrogen) containing 5% fetal bovine serum (Thermo Scientific). Following incubation for 24 hours at 37°C (in 5% CO_2), the medium was removed and serial dilutions of antibody were added. Luciferase activity was determined by using a Bright-Glo luciferase assay kit (Promega) after 72 hours according to the manufacturer's instructions. The results were calculated as the average percentage relative to the reactivity in untreated cells, which was set at 100%. The viability of the replicon cells was measured by using a WST-8 cell counting kit (Dojindo) according to the manufacturer's instructions.

Immunostaining and Antibodies

Cells were cultured on glass coverslips (1.0 cm diameter) and fixed with 1% paraformaldehyde in phosphate-buffered saline (PBS) at room temperature for 10 minutes in 24-well plates. To permeabilize the cell membranes, the cells were treated with 1% Triton X-100 in PBS at room temperature for 10 minutes. After washing with 0.05% Tween-20 in PBS, the cells were incubated with 2-152a MAb, antiprotein disulfate isomerase (PDI) rabbit polyclonal antibody (Stressgen Bioreagents) or normal mouse IgG for 1 hour and washed with 0.05% Tween-20 in PBS. Alexa Fluor 488-labeled goat antimouse IgG was used as the secondary antibody.

Anti-NS5A antibody was provided by Dr Yoshiharu Matsuura (Osaka University). Anti-myc mouse monoclonal antibody

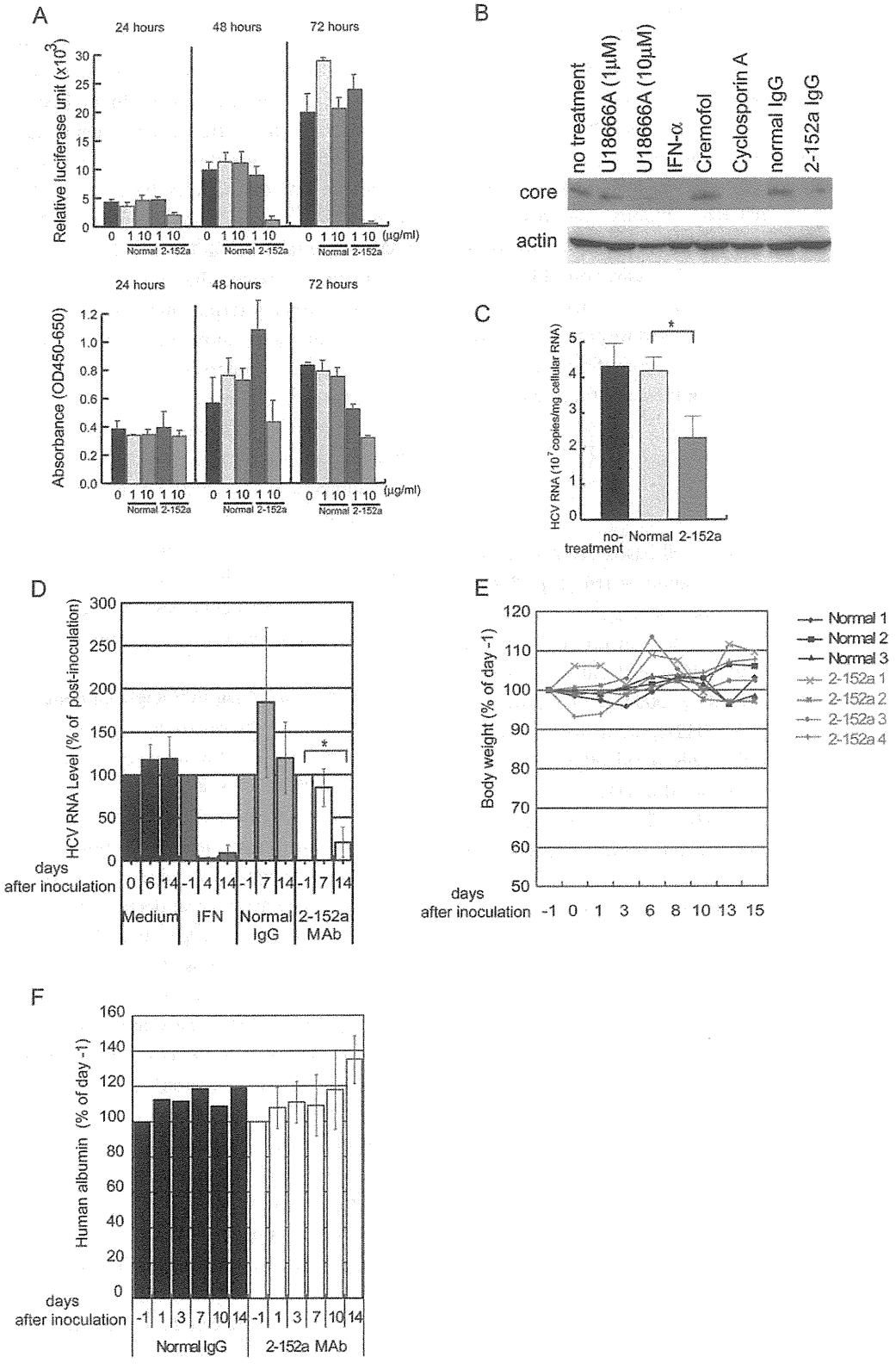

Figure 1. Anti-DHCR24 monoclonal antibody (2-152a MAb) suppresses HCV replication in vitro and in vivo. *A*, The effects of 2-152a MAb on HCV replication were measured by the luminescence activity and cell viability in FLR3-1 cells. The replicon cell line was incubated with IgG from normal mice or 2-152a MAb at 1 or 10 μg/mL for 24, 48, and 72 hours. The mean values from triplicate wells are indicated, and the vertical bars represent the standard deviation. The medium control (2% FCS-DMEM) without IgG is indicated as 0. *B*, The JFH/K4 cells were treated with cholesterol synthesis inhibitor U18666A (1 mM, 10 mM), IFN-α (250 IU/mL), Cyclosporin A (25 μM) and its solvent Cremophor, normal mouse IgG (10 μg/mL), and 2-152a IgG (10 μg/mL). HCV core and actin proteins were detected. *C*, HCV RNA copies were measured in JFH/K4 cells after treatment with normal or 2-152a IgG

(9E10; Cell Signaling Technology) and antiactin mouse monoclonal antibodies (Sigma-Aldrich) were utilized for detecting myc-fusion protein and normalization of the results, respectively.

cDNA Synthesis and Quantitative Reverse Transcriptase PCR

cDNA was synthesized from 0.5 or 1 mg of total RNA with a Superscript II kit (Invitrogen). TaqMan gene expression assays were custom designed and manufactured by Applied Biosystems. The expression was quantified with the ABI 7500 real-time PCR system (Applied Biosystems).

Microarray Analysis

For microarray analysis, total RNAs were extracted using RNAeasy kit (Qiagen), and RNA integrity was assessed using a Bioanalyzer (Agilent Technologies). cRNA targets were synthesized and hybridized with Whole Human Genome Oligo Microarray (G4112F; Agilent) according to the manufacturer's instructions.

RNA Interference, Expression Vector Construction, Transfection, and Rescue Experiments

Small interference RNA (siRNA) targeting betaine/GABA transporter-1 (BGT-1; nucleotides 120–144) was designed by using a program (https://rnaidesigner.invitrogen.com/) based on registered sequences in GenBank (5′-CAACAAGATGGAGT TTGTGCTGTCA-3′). Alternative siRNA (BGT-1-siRNA-362; nucleotides 362–386) was similarly designed. The HCV-siRNA (R7) sequence was 5′-GUCUCGUAGACCGUGCACCA dTdT-3′.

The coding region of the BGT-1 gene was obtained from RNA of R6FLR-N cells by reverse transcription–polymerase chain reaction (RT-PCR). The PCR products were inserted in *Eco*RV–*Xho*I sites of pcDNA6-myc His, version A (Invitrogen) after digestion of *Eco*RV–*Xho*I. To generate mutant plasmids that contained nucleotide substitutions in the siRNA-targeted site, we introduced point mutations into pcDNA-BGT-1 by using site-directed mutagenesis with a QuickChange multisite-directed mutagenesis kit (Stratagene), according to the manufacturer's instructions, and the following oligonucleotide primer: BGT-1-mut, 5′-CCAATGGACCAA-CAAGATGGAATTCGTTCTATCGGTGGCCGGGGAGCTC ATTGGG-3′ (the mutations introduced by mutagenesis are underlined).

Transfection of siRNAs was carried out by reverse transfection using Lipofectamine RNAiMAX according to the manufacturer's protocol (Invitrogen). Transfection of the expression vector was undertaken by using Lipofectamine LTX with Plus reagent (Invitrogen).

The rescue experiment was performed after reverse transfection of BGT-1 siRNA (1.5 nM) into R6FLR-N cells by using RNAiMAX reagent. After 48 hours, wild-type (wt) and mutant (mut) BGT-1 expression vectors (10 ng) were transfected by using Lipofectamine LTX, and the luciferase activity and cell viability were assessed by WST-8 assay (Dojindo) after 24 hours.

Analysis of HCV Infection and BGT-1 Expression

For infection assays, Cured/HuH-7 K4 cells were incubated with JFH/K4 cell-derived HCV (2.0×10^6 copies/mL). At 72 hours after incubation, HCV infection and BGT-1 expression were analyzed by real-time detection (RTD)-PCR and TaqMan expression assay, respectively, as described earlier.

Statistical Analysis

The Student t test was used to test the statistical significance of the results. P values $< .05$ were considered statistically significant.

Results

Inhibitory Effect of 2-152a MAb on HCV Replication In Vitro

We examined the effects of 2-152a MAb on HCV replication and the viability in HCV replicon cell lines. The treatment with 2-152a MAb significantly decreased HCV replication after 48 hours and cell viability after 72 hours (Figure 1*A*). To determine the recognition site of 2-152a MAb, we performed epitope mapping by using serial overlapping deletion mutants of the DHCR24 fusion protein (Supplementary Figure 1*A*). The recognition site was identified within amino acid residues 259–314 (Supplementary Figure 1*B*) and the predicted "Diminuto-like protein" homologous region [23] indicated in Supplementary Figure 1A.

Suppression of HCV Infection by 2-152a MAb

To determine the effects of 2-152a MAb on HCV infection, we inoculated the antibody into a persistently HCV-infected cell line (JFH/K4; Figure 1*B* and *C*) or uPA-SCID chimeric mice previously transplanted with human hepatocytes [20] and

Figure 1 continued. (10 μg/mL). The error bars indicate the standard deviation, and the asterisk indicates $P < .005$. *D*, Relative amounts of HCV RNA (% copies/mg total RNA on days −1 or 0) in the livers of chimeric mice inoculated with the control medium, PEGylated IFN-α, normal IgG, or 2-152a IgG were estimated by RTD-PCR. For normalization, the HCV RNA level 1 day before the inoculation (day −1) or on the day of inoculation (day 0) was defined as 100%. The graph shows the relative amounts of HCV RNA at −1 day (or day 0), 7 days (or 4 days), and 14 days. The error bars indicate the standard deviation, and the asterisk indicates $P < .005$. *E*, Ratio of body weight of mice inoculated with either normal IgG or 2-152a MAb IgG to that on day −1. *F*, Ratio of albumin concentration in serum samples of mice inoculated with 2-152a MAb IgG or normal IgG to that on day −1. The vertical bars indicate the standard deviation.

A

R6 2-152a 24h Gene Name	2-152a/normal IgG
CNN1	2.63
A_24_P398370	2.57
ACTA1	2.44
CSTA	1.71
ENST00000298047	1.7
TAGLN	1.63
AI379175	1.6
MGAM	1.58
MSRB3	1.57
MSRB3	1.56
EPPK1	1.47
THC2317432	1.45
AK055214	1.43
SLC16A6	1.39
AKR1C1	0.75
AKR1C1	0.74
CD44	0.74
CD44	0.73
ARG1	0.72
F2RL2	0.72
CYP3A7	0.71
CD44	0.7
LOC642775	0.7
S100A4	0.68
SLC7A8	0.67
VNN2	0.65
ROBO3	0.65
CDKN1C	0.63
FUT3	0.61
KCNMA1	0.6
BGT-1	0.58

FLR3-1 2-152a 24h Gene Name	2-152a/normal IgG
CNN1	2.18
ACTA1	1.98
SLC16A14	1.59
CSTA	1.52
LYPD1	1.51
IL11	1.51
KCNJ8	1.41
MSRB3	1.4
C8orf4	1.4
PPP3R1	1.39
ELF5	0.73
CYP3A7	0.72
COL14A1	0.71
LOC401022	0.71
THC2437143	0.7
BG542103	0.7
S100A4	0.7
PTGS1	0.69
F2RL2	0.68
FUT5	0.67
FCGBP	0.66
FUT3	0.64
PTGS1	0.64
SLC6A14	0.63
CNN2	0.63
THC2442210	0.63
ZNF114	0.62
SMPD3	0.61
BGT-1	0.58
CDKN1C	0.49

FLR3-1 2-152a 72h Gene Name	2-152a/normal IgG
CGA	1.54
TAGLN	1.47
CNN1	1.39
RSNL2	0.75
SLC37A2	0.74
AKR1C1	0.73
BG542103	0.72
PTGS1	0.71
THC2437143	0.71
AKR1B10	0.71
SLC6A14	0.70
AKR1B10	0.70
COL14A1	0.69
SLC6A14	0.69
SMPD3	0.67
VNN2	0.66
FXYD2	0.65
F2RL2	0.62
BGT-1	0.61
FXYD2	0.59
FLJ25422	0.42

K4 2-152a 24h Gene Name	2-152a/normal IgG
KIAA0367	1.97
ACTA1	1.90
CNN1	1.88
A_24_P398370	1.81
SLC16A14	1.80
ADH1A	1.59
ROBO2	1.56
AKR1D1	1.54
SLC17A1	1.50
SLC16A14	1.47
BC036599	1.46
TAGLN	1.44
MSRB3	1.43
SOCS2	1.37
FXYD2	0.74
ENST00000036	0.73
SLC7A8	0.72
ARG2	0.72
IGFBP5	0.71
ROBO3	0.71
GPX2	0.70
CR603668	0.70
IGFBP5	0.69
COL14A1	0.69
AF118081	0.68
VNN2	0.67
HOXD1	0.66
CDKN1C	0.66
THC2442210	0.66
LOC647022	0.65
COL14A1	0.62
SLC6A14	0.53
FUT3	0.53

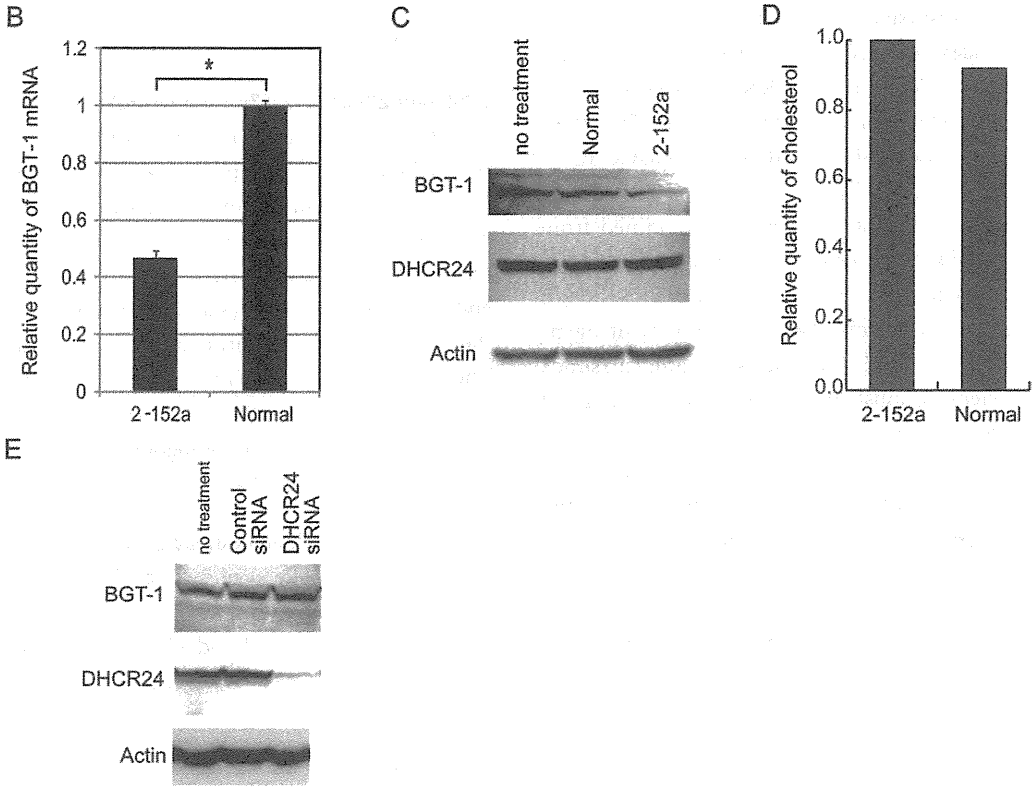

Figure 2. *A*, Genes that showed significant changes in expression after the 2-152a MAb treatment. HCV replicon cells (FLR3-1 and R6FLR-N) and K4 cells were treated with 2-152a MAb. The symbols shaded in gray indicate the genes that showed significantly changed expression commonly in R6FLR-N and FLR3-1 cells, and those shaded in orange indicate the genes that showed significantly changed expression in K4 cells. The amount of labeled probe for microarray analysis was 7-fold higher than that in the first experiment (Supplementary Table 1). Each value indicates the number of ratios of signal 2-152a MAb/normal IgG treatment. *B*, TaqMan expression assay of BGT-1 in samples of R6FLR-N cells treated with 2-152a MAb or normal IgG. BGT-1 mRNA (0.5 μg) samples treated with 2-152a MAb or normal IgG were transcribed by reverse transcriptase, and synthesized cDNAs were used for TaqMan